Supporting Information

Probes and Dyes Design through Copper-mediated Reactions of *N*-arylhydroxylamines

Xiaotong Xia[a,c], Shuru Liu[a,c], Wenming Liu[b,c],Qiuying Xu[a], Ximing Xu[d], Fang Liu[b,*], Tao Deng[a,c,*]

[a]*Lingnan Medical Research Center, The first Affiliated Hospital of Guangzhou University of Chinese Medicine, Guangzhou, 510006, PR China*
[b]*School of Pharmaceutical Sciences, Guangzhou University of Chinese Medicine, Guangzhou, 510006, PR China*
[c]*Artemisinin Research Center, Guangzhou University of Chinese Medicine, Guangzhou, 510006, PR China*
[d]*School of Medicine and Pharmacy, Ocean University of China, Qingdao 266071, Shandong, China*

Contents

1. Reagents and apparatus

Chemicals were purchased from commercial sources, all reagents were AR grade and used without further purification. The distilled deionized water from a Milli-Q Plus system was used throughout the experiments. A high-performance liquid chromatography (Agilent HPLC 1260, USA) system and a reverse phase C18 column (250 x 4.6 mm) were applied when needed. Photo-reductive reaction was carried out by a photochemical reactor (WATTCAS, Xi'an). Fluorescence reading was performed by a Varioskan LUX plate reader (Thermo Fisher) supplied with the software SkanIt 4.1. High resolution mass (HRMS) was collected from a Triple TOF5600 system (SCIEX). ICP-MS was collected on an Agilent 7700ICP-MS. Fluorescence lifetime was measured by a Fluoro Max-4 (HORIBA Scientific). ^{1}H and ^{13}C NMR spectra were recorded on AVANCE III HD 400 MHz and ASCEND™ 400 MHz digital NMR spectrometer (Switzerland). Data was reported as follows: chemical shift, multiplicity (s = singlet, d = doublet, and m = multiplet), coupling constant (*J* values) in Hz and integration.

2. Synthesis and characterization

2.1 General procedure for compound 3

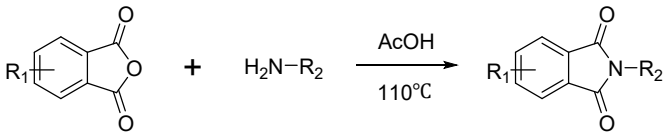

1 **2** **3**

R_1 = NO_2, OH
R_2 = n-Bu, Me

Compound **1** (2 mmol) was dissolved in 5 mL acetic acid, amine **2** (3mmol) was then added drop wise into the solution under stirring. The reaction was performed at 110°C for 2 h. When the reaction mixture was cooled to room temperature, cool water was added. The precipitates were collected and washed with cool water, and then dried against a vacuum to give the products.

2.2 General procedure for compound 4[1]

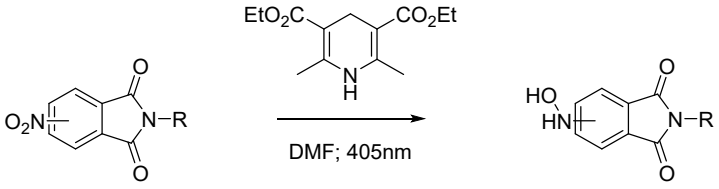

3 **4**

R = n-Bu, Me

Compound **3** (1 mmol) and diethyl 2,6-dimethyl-1,4-dihydropyridine-3,5-dicarboxylate (Hantzsch ester, 1.0-4.0 mmol) were dissolved in 4 mL DMF in a round bottom reaction tube. The tube was then placed into the photochemical reactor and irradiated with a 5W blue LED (λ_{max} = 405 nm). The reaction was monitored by TLC until **3** is completely consumed. Distilled water was added, the solution was then extracted with ethyl acetate twice, the organic layer was then washed with saturated NaCl solution and dried over anhydrous Na_2SO_4. The organic layer was concentrated by a rotary evaporator and then purified by silica gel column chromatography using the mixture of methanol/dichloromethane as the eluent.

2.3 General procedure for compound 5

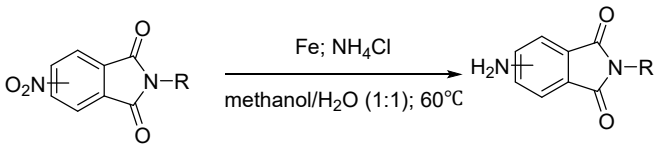

3 **5**

R = n-Bu, Me

Ferrous powder (5eq) was added into the mixture of **3** (1eq, 1 mmol) and ammonium chloride (10 eq, 10 mmol) in methanol/H_2O (1:1). The reaction was performed at 60°C for 2 hours, and then cooled to room temperature. The mixture was filtered, the filtrate was collected. After removal of methanol under reduced pressure, the resulting aqueous fraction was adjusted to pH 4 with 2M HCl and then extracted with ethyl acetate. The organic layer was washed with saturated NaCl and dried over anhydrous Na_2SO_4. After concentrated under reduced pressure, the crude residue was purified by silica gel flash column chromatography using the mixture of methanol/dichloromethane as the eluent.

2.4 General procedure for compound 7

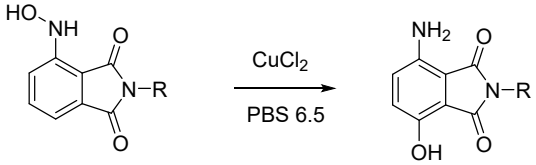

4 **7**

R = n-Bu, Me

Compound **4** (0.2 mmol) and $CuCl_2$ (0.02 mmol) was dissolved in 20 mL PBS buffer (pH 6.5). The mixture was stirred at 50 °C for 6 hours. The reaction mixture was then extracted three times

with ethyl acetate. After washing with brine, the organic fraction was dry against Na_2SO_4. The crude residue was purified by silica gel flash column chromatography using the mixture of methanol/dichloromethane as the eluent.

2.5 General procedure for compound 8

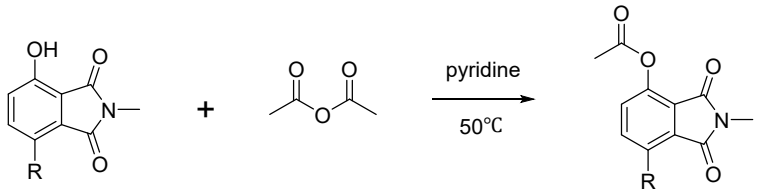

3d or 7b

R = H, NH_2

8

Compound **3d** or **7b** (1eq, 0.3 mmol) was dissolved in 4 mL pyridine at 0 °C. Acetic anhydride (1.2eq, 0.36 mmol) was added drop wise to the solution. After stirring at 0°C for 5min, the reaction mixture was heated to 50°C. One hour later, ice water was added, the mixture was then extracted twice with ethyl acetate. The organic layer was dried with anhydrous Na_2SO_4.The purified product was obtained by silica gel flash column chromatography dichloromethane/methanol = 100/1).

2.6 Synthesis of 4-amino-7-methoxy-2-methylisoindoline-1,3-dione (9)

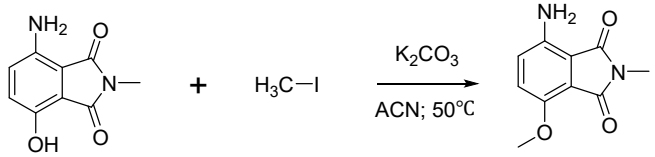

7b **9**

Compound **7b** (21mg, 0.11 mmol) was dissolved in 5 mL-acetonitrile, iodomethane (78 mg, 0.55 mmol) was then added while stirring, followed by finely powdered K_2CO_3 (30 mg, 0.22 mmol). After stirring at 50°C for 10 hours, the mixture was cooled and the solvent was removed. The crude product was purified by silica gel column chromatography dichloromethane/methanol= 100/1) to give **9** 5.2 mg (23%yield).

2.7 Synthesis of N-(7-hydroxy-2-methyl-1,3-dioxoisoindolin-4-yl)acetamide (10)

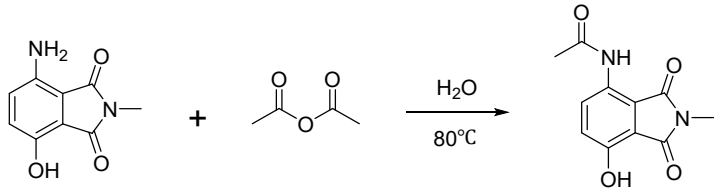

7b **10**

Compound **7b** (0.16 mmol) was dissolved in 5 mL distilled deionized water. Acetic anhydride

(500 μL) was added drop wise to the solution. The reaction was stirred at 80°C for 20 hours and then cooled to room temperature. Distilled water was added and the mixture was extracted with ethyl acetate. The organic layer was separated and dried over anhydrous Na_2SO_4. After concentrating under vacuum, the crude product was purified by silica gel column chromatography (dichloromethane/methanol = 100/1) to give **10** 14.3 mg (39% yield).

2.8 Synthesis of N-(2-methyl-1,3-dioxoisoindolin-4-yl)acetamide (11)

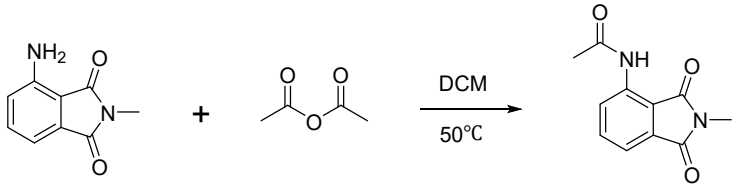

5c **11**

Compound **5b** (30 mg, 0.17 mmol) was added into 5 mL dried dichloromethane followed by the addition of acetic anhydride (300 μL). The mixture was then heated to 50°C by a heating mantle and stirred at this temperature for 15 h. When the reaction mixture was cooled to room temperature, the solvent was removed and the crude product was purified by silica gel column chromatography (dichloromethane/methanol = 200/1) to give **11** (30.1 mg, 82% yield).

3. Characterization of compounds

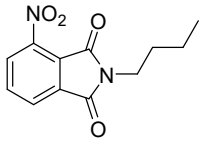

2-butyl-4-nitroisoindoline-1,3-dione (3a): white solid, 80% yield; ^{1}H NMR (400 MHz, $CDCl_3$) δ 8.13 – 8.06 (m, 2H), 7.93 – 7.87 (m, 1H), 3.73 – 3.70 (m, 2H), 1.71 – 1.62 (m, 2H), 1.39– 1.32 (m, 2H), 0.96 – 0.93 (m, 3H).^{13}C NMR (100 MHz, $CDCl_3$) δ 165.97, 163.06, 145.09, 135.39, 134.22, 128.49, 126.99, 123.84, 38.56, 30.40, 20.08, 13.61.HRMS (ESI) m/z: $[M+H]^+$ Calcd for $C_{12}H_{12}N_2O_4H^+$ 249.0870; Found 249.0867.

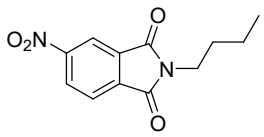

2-butyl-5-nitroisoindoline-1,3-dione (3b): white solid, 81% yield; ^{1}H NMR (400 MHz, $CDCl_3$) δ 8.65 (d, J = 1.8 Hz, 1H), 8.61– 8.58 (m, 1H), 8.03 (d, J = 8.1 Hz, 1H), 3.76 – 3.72 (m, 2H), 1.73 – 1.63 (m, 2H), 1.42 – 1.32 (m, 2H), 0.97 – 0.93 (m, 3H). ^{13}C NMR (100 MHz, $CDCl_3$) δ 166.40, 166.11, 151.84, 136.71, 133.68, 129.29, 124.48, 118.71, 38.64, 30.56, 20.16, 13.69. HRMS (ESI) m/z: $[M+H]^+$ Calcd for $C_{12}H_{12}N_2O_4H^+$ 249.0870; Found 249.0869.

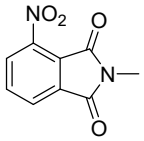

2-methyl-4-nitroisoindoline-1,3-dione (3c): white solid, 57% yield; ^{1}H NMR (400 MHz, $CDCl_3$) δ 8.09– 8.06 (m, 2H), 7.93– 7.89 (m, 1H), 3.16 (s, 3H). ^{13}C NMR (100 MHz, $CDCl_3$) δ 165.83, 163.02, 144.82, 135.46, 134.07, 128.39, 126.92, 123.72, 24.44. HRMS (ESI) m/z: $[M+H]^+$ Calcd for $C_9H_6N_2O_4H^+$ 207.0400; Found 207.0400.

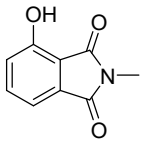

4-hydroxy-2-methylisoindoline-1,3-dione (3d, PHI-1): white solid, 63% yield; ^{1}H NMR (400 MHz, *d6*-DMSO) δ 10.95 (s, 1H), 7.59– 7.55 (m, 1H), 7.25– 7.23 (m, 1H), 7.19– 7.16 (m, 1H), 2.95 (s, 3H). ^{13}C NMR (100 MHz, *d6*-DMSO) δ 167.83, 166.79, 154.97, 135.73, 133.77, 123.07, 114.86, 113.82, 23.42. HRMS (ESI) m/z: $[M+H]^+$ Calcd for $C_9H_7NO_3H^+$178.0499; Found 178.0488.

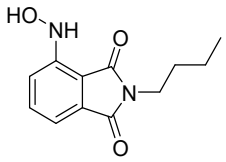

2-butyl-4-(hydroxyamino)isoindoline-1,3-dione (4a, P1): yellow solid, 40% yield; ^{1}H NMR (400 MHz, $(CD_3)_2CO$) δ 8.56 (s, 1H), 8.41 (s, 1H), 7.67 – 7.64 (m, 1H), 7.50 (d, J = 8.4 Hz, 1H), 7.21 (d, J = 7.1 Hz, 1H), 3.60 – 3.57 (m, 2H), 1.65– 1.58 (m, 2H), 1.39 – 1.29 (m, 2H), 0.95 – 0.91 (m, 3H). ^{13}C NMR (100 MHz, $(CD_3)_2CO$) δ 168.98, 168.03, 149.02, 135.30, 132.52, 118.56, 113.43, 111.90, 36.93, 30.46, 19.76, 13.02. HRMS (ESI) m/z: $[M+H]^+$ Calcd for $C_{12}H_{14}N_2O_3H^+$235.1077; Found 235.1079.

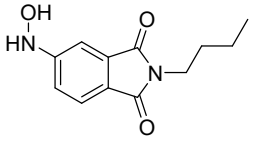

2-butyl-5-(hydroxyamino)isoindoline-1,3-dione (4b, P2): light orange solid, 95% yield; ^{1}H NMR (400 MHz, $CDCl_3$) δ 7.69 (d, J = 8.1 Hz, 1H), 7.44 (d, J = 1.6 Hz, 1H), 7.20 – 7.13 (m, 2H), 5.98 (s, 1H), 3.66 – 3.62 (m, 2H), 1.67 – 1.58 (m, 2H), 1.39– 1.30 (m, 2H), 0.95 – 0.91 (m, 3H). ^{13}C NMR (100 MHz, $CDCl_3$) δ 168.85, 168.60, 155.70, 134.30, 124.52, 124.49, 117.42, 108.17, 37.91, 30.82, 20.22, 13.79. HRMS (ESI) m/z: $[M+H]^+$ Calcd for $C_{12}H_{14}N_2O_3H^+$ 235.1077; Found 235.1077.

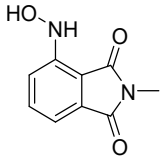

4-(hydroxyamino)-2-methylisoindoline-1,3-dione (4c): yellow solid, 55% yield; ^{1}H NMR (400 MHz, *d6*-DMSO) δ 9.06 (d, J = 1.4 Hz, 1H), 8.89 (s, 1H), 7.64– 7.60 (m, 1H), 7.37 (d, J = 8.4 Hz, 1H), 7.15 (d, J = 7.1 Hz, 1H), 2.97 (s, 3H). ^{13}C NMR (100 MHz, *d6*-DMSO) δ 168.40, 168.19, 148.61, 135.50, 132.33, 118.07, 112.73, 110.63, 23.38. HRMS (ESI) m/z: $[M+Na]^+$ Calcd for $C_9H_8N_2O_3Na^+$ 215.0427; Found 215.0428.

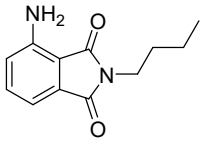

4-amino-2-butylisoindoline-1,3-dione (5a): yellow oil, 80% yield; ^{1}H NMR (400 MHz, *d6*-DMSO) δ 7.42– 7.38 (m, 1H), 6.98 – 6.91 (m, 2H), 6.42 (s, 2H), 3.50 – 3.46 (m, 2H), 1.55– 1.48 (m, 2H), 1.28 – 1.21 (m, 2H),0.89 – 0.85 (m, 3H). ^{13}C NMR (100 MHz, *d6*-DMSO) δ 169.60, 168.19, 146.47, 135.13, 132.42, 121.43, 110.71, 109.02, 36.58, 30.20, 19.57, 13.57. HRMS (ESI) m/z: $[M+H]^+$ Calcd for $C_{12}H_{14}N_2O_2H^+$ 219.1128; Found 219.1123.

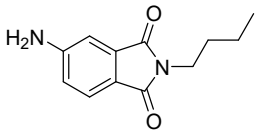

5-amino-2-butylisoindoline-1,3-dione (5b): light yellow solid, 68.2% yield; ^{1}H NMR (400 MHz, d6-DMSO) δ 7.46 (d, J = 8.2 Hz, 1H), 6.90 (d, J = 2.0 Hz, 1H), 6.79 – 6.76 (m, 1H), 6.44 (s, 2H), 3.48 – 3.45 (m, 2H), 1.56 – 1.45 (m, 2H), 1.29 – 1.19 (m, 2H), 0.89 – 0.85 (m, 3H). ^{13}C NMR (100 MHz, d6-DMSO) δ 168.34, 168.04, 154.92, 134.45, 124.79, 116.60, 116.50, 106.94, 36.64, 30.20, 19.50, 13.50. HRMS (ESI) m/z: $[M+H]^+$ Calcd for $C_{12}H_{14}N_2O_2H^+$ 219.1128; Found 219.1122

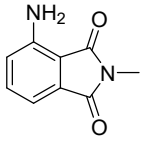

4-amino-2-methylisoindoline-1,3-dione (5c, PHI-2): light yellow solid, 83% yield; ^{1}H NMR (400 MHz, *d6*-DMSO) δ 7.42– 7.38 (m, 1H), 6.98 – 6.91 (m, 2H), 6.41 (s, 2H), 2.95 (s, 3H). ^{13}C NMR (100 MHz, *d6*-DMSO) δ 169.59, 168.24, 146.31, 134.99, 132.58, 121.30, 110.61, 109.23, 23.23. HRMS (ESI) m/z: $[M+K]^+$ Calcd for $C_9H_8N_2O_2K^+$ 215.0217; Found 215.0223.

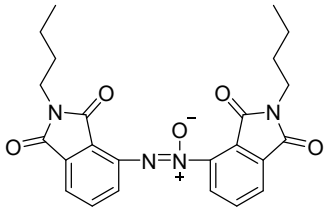

1,2-bis(2-butyl-1,3-dioxoisoindolin-4-yl)diazene 1-oxide (6a): light orange solid, 19.7% yield; ^{1}H NMR (400 MHz, $CDCl_3$) δ 8.26 – 8.24 (m, 1H), 8.12 – 7.81(m, 5H), 3.77 – 3.65 (m, 4H), 1.71 – 1.61 (m, 4H), 1.47 – 1.30 (m, 4H), 0.97 – 0.91 (m, 6H). ^{13}C NMR (100 MHz, $CDCl_3$) δ 168.03, 166.79, 166.63, 164.35, 148.33, 144.04, 140.06, 135.48, 135.13, 133.71, 133.26, 129.03, 127.97, 126.00, 125.41, 123.80, 123.45, 122.72, 121.86, 38.50, 38.09, 30.73, 30.59, 20.24, 20.22, 13.77, 13.73. HRMS (ESI) m/z: $[M+H]^+$ Calcd for $C_{24}H_{24}N_4O_5H^+$ 449.1820; Found 449.1813.

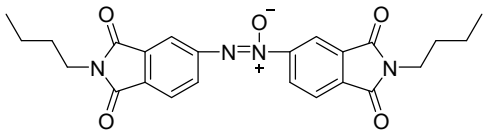

1,2-bis(2-butyl-1,3-dioxoisoindolin-5-yl)diazene 1-oxide (6b): light yellow solid, 31.4% yield; ^{1}H NMR (400 MHz, $CDCl_3$) δ 8.80 (d, J = 1.9 Hz, 1H), 8.76 – 8.69 (m, 2H), 8.36 – 8.34 (m, 1H), 8.03 (d, J = 8.2 Hz, 1H), 7.97 (d, J = 8.1 Hz, 1H), 3.77 – 3.71 (m, 4H), 1.73 – 1.66 (m, 4H), 1.43 – 1.35 (m, 4H), 0.99 – 0.95 (m, 6H). ^{13}C NMR (100 MHz, $CDCl_3$) δ 167.54, 167.44, 166.83, 166.67, 151.86, 147.70, 134.88, 133.31, 133.09, 132.48, 131.52, 128.17, 124.06, 123.88, 119.68, 117.83, 38.40, 38.14, 30.61, 30.53, 20.10, 20.09, 13.65, 13.62. HRMS (ESI) m/z: $[M+H]^+$Calcd for $C_{24}H_{24}N_4O_5H^+$ 449.1820; Found 449.1818.

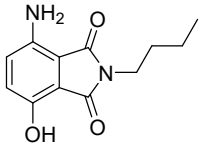

4-amino-2-butyl-7-hydroxyisoindoline-1,3-dione (7a): yellow oil, 21% yield; ^{1}H NMR (400 MHz, *d6*-DMSO) δ 9.89 (s, 1H), 6.96 (d, J = 9.0 Hz, 1H), 6.89 (d, J = 9.0 Hz, 1H), 5.96 (s, 2H), 3.46 – 3.43 (m, 2H), 1.54– 1.47 (m, 2H), 1.29 – 1.19 (m, 2H), 0.89 – 0.85 (m, 3H).^{13}C NMR (100 MHz, *d6*-DMSO) δ 168.99, 166.59, 146.12, 140.21, 126.36, 124.77, 112.51, 108.18, 36.18, 30.19, 19.50, 13.52. HRMS (ESI) m/z: $[M+H]^+$ Calcd for $C_{12}H_{14}N_2O_3H^+$235.1077; Found 235.1071.

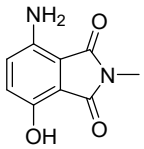

4-amino-7-hydroxy-2-methylisoindoline-1,3-dione (7b, PHI-3): orange solid, 22% yield; ^{1}H NMR (400 MHz, *d6*-DMSO) δ 9.88 (s, 1H), 6.96 (d, J = 9.0 Hz, 1H), 6.88 (d, J = 9.0 Hz, 1H), 5.95 (s, 2H), 2.91 (s, 3H). ^{13}C NMR (100 MHz, *d6*-DMSO) δ 169.04, 166.68, 146.02, 140.13, 126.26, 124.70, 112.72, 108.43, 22.99. HRMS (ESI) m/z: $[M+H]^+$ Calcd for $C_9H_8N_2O_3H^+$ 193.0601; Found 193.0601.

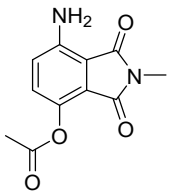

7-amino-2-methyl-1,3-dioxoisoindolin-4-yl acetate (8a, PHI-4): yellow solid, 43% yield; ^{1}H NMR (400 MHz, *d6*-DMSO) δ 7.15 (d, J = 9.0 Hz, 1H), 6.99 (d, J = 8.9 Hz, 1H), 6.43 (s, 2H), 2.92 (s, 3H), 2.27 (s, 3H).^{13}C NMR (100 MHz, *d6*-DMSO) δ 168.91, 168.75, 165.73, 144.52, 135.69, 130.18, 123.11, 121.92, 108.76, 23.24, 20.41. HRMS (ESI) m/z: $[M+H]^+$ Calcd for $C_{11}H_{10}N_2O_4H^+$ 235.0713; Found 235.0707.

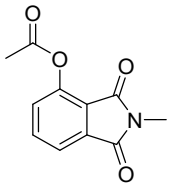

2-methyl-1,3-dioxoisoindolin-4-yl acetate (8b, PHI-6): white solid, 80% yield; ^{1}H NMR (400 MHz, $CDCl_3$) δ 7.75 – 7.68 (m, 2H), 7.35– 7.32 (m, 1H), 3.13 (s, 3H), 2.42 (s, 3H). ^{13}C NMR (100 MHz, $CDCl_3$) δ 168.68, 167.56, 166.11, 146.49, 135.63, 133.83, 128.25, 123.07, 120.88, 23.94, 20.68.HRMS (ESI) m/z: $[M+H]^+$ Calcd for $C_{11}H_9NO_4H^+$220.0604; Found 220.0599.

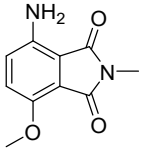

4-amino-7-methoxy-2-methylisoindoline-1,3-dione (9, PHI-5): yellow solid, 23% yield; ^{1}H NMR (400 MHz, *d6*-DMSO) δ 6.81 (d, J = 9.1 Hz, 1H), 6.58 (d, J = 9.1 Hz, 1H), 5.63 (s, 2H), 3.40 (s, 3H), 2.50 (s, 3H). ^{13}C NMR (100 MHz, *d6*-DMSO) δ 169.01, 166.11, 147.47, 140.90, 124.30, 122.36, 115.49, 109.41, 56.51, 23.10.HRMS (ESI) m/z: $[M+H]^+$ Calcd for $C_{10}H_{10}N_2O_3H^+$ 207.0764; Found 207.0768.

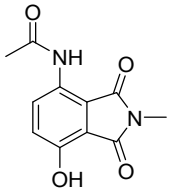

N-(7-hydroxy-2-methyl-1,3-dioxoisoindolin-4-yl)acetamide (10, PHI-7): light yellow solid, 48% yield; ^{1}H NMR (400 MHz, *d6*-DMSO) δ 10.81 (s, 1H), 9.53 (s, 1H), 8.17 (d, J = 9.1 Hz, 1H), 7.14 (d, J = 9.1 Hz, 1H), 2.94 (s, 3H), 2.11 (s, 3H). ^{13}C NMR (100 MHz, *d6*-DMSO) δ 168.64, 168.20, 166.16, 151.05, 128.79, 128.61, 124.53, 118.63, 113.63, 24.03, 23.34. HRMS (ESI) m/z: $[M+H]^+$ Calcd for $C_{11}H_{10}N_2O_4H^+$ 235.0713; Found 235.0711.

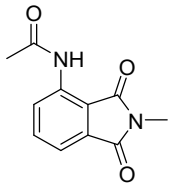

N-(2-methyl-1,3-dioxoisoindolin-4-yl)acetamide (11, PHI-8): white solid, 81% yield; ^{1}H NMR (400 MHz, *d6*-DMSO) δ 9.60 (s, 1H), 8.38 (d, J = 8.3 Hz, 1H), 7.72– 7.68 (m, 1H), 7.48 (d, J = 7.2 Hz, 1H), 2.99 (s, 3H), 2.18 (s, 3H). ^{13}C NMR (100 MHz, *d6*-DMSO) δ 169.62, 169.08, 167.94, 136.59, 135.89, 132.35, 125.69, 118.14, 117.54, 24.70, 23.99. HRMS (ESI) m/z: $[M+H]^+$ Calcd for $C_{11}H_{10}N_2O_3H^+$ 219.0764; Found 219.0755.

4. Supplementary data

4.1 Summary of recent studies on copper ions fluorescence detection.

Table S1. A list of recently published fluorescence detection systems for copper ions

Probe	Substrate	Mechanism	Linear range	LOD	Selevtivity and anti-interference	Ref.
FLCS1	Cu^{+}	Chelation; PET inhibition			Slightly influenced by Cu^{2+}	[2]
GdL_1	Cu^{2+}	Chelation; affinity to HSA			Slightly influenced by Zn^{2+}	[3]
NDQI	Cu^{2+}	Chelation; ICT inhibition	0.31-50μM	20 nM	ROS influence	[4]
CUSP	Cu^{+}/Cu^{2+}	Chelation	0.50-10 μM	Cu^{+} : 42nM Cu^{2+} : 34nM;	Remarkable selectivity	[5]
ZPSN	Cu^{+}	Chelation; intramolecular ET inhibition	0-10 μM	8.2 nM	Hg^{2+}influence	[6]
DDP-Cu	Cu^{2+}	Cu^{2+}-catalyzed hydrolysis; ICT recovery	0-10 μM	36 nM	Remarkable selectivity	[7]
NIR-Cu	Cu^{2+}	Cu^{2+}-catalyzed hydrolysis	1-5 μM	29 nM	Remarkable selectivity	[8]
1(naphthalimide -rhodamine)	Cu^{2+}	Cu^{2+}-catalyzed hydrolysis; FRET recovery	0-16μM	18.6nM	Low interference	[9]
1 (hydrazide-naphthalimide)	Cu^{2+}	Cu^{2+}-catalyzed hydrolysis;	0-25μM	1.1 μM	Remarkable selectivity	[10]
OAHP	Cu^{2+}	oxidative Decomposition andintramolecular	0.05-2μM	18 nM	Remarkable selectivity	[11]

1(hemicyanine-pyridinecarbonyl)	Cu^{2+}	cyclization Cu^{2+}-catalyzed hydrolysis; ICT recovery	0.02-8μM	4.0 nM	Remarkable selectivity	[12]
P1	Cu^{2+}/Cu^{+}	Cleavage and rearrangement	0.125-20 μM;	Cu^{2+}: 1.11nM	Remarkable selectivity	This work

4.2 Copper ions detection by the newly synthetic probes.

The detection was performed mainly on Cu^{2+} since free Cu^{+} normally has stability issues in ambient atmospheric conditions. A typical detection was performed at 50 °C for 100 min in PBS buffer (pH 6.5). In the final detection solution, the concentration of P1 was set at 100 μM. The fluorescence intensity at the wavelength of 511 nm was collected upon 390 nm excitation. $CuCl_2$ and CuCl were used as the source of Cu^{2+} and Cu^{+} throughout the study unless otherwise noted. Data are presented as the mean ± SD (n = 3).

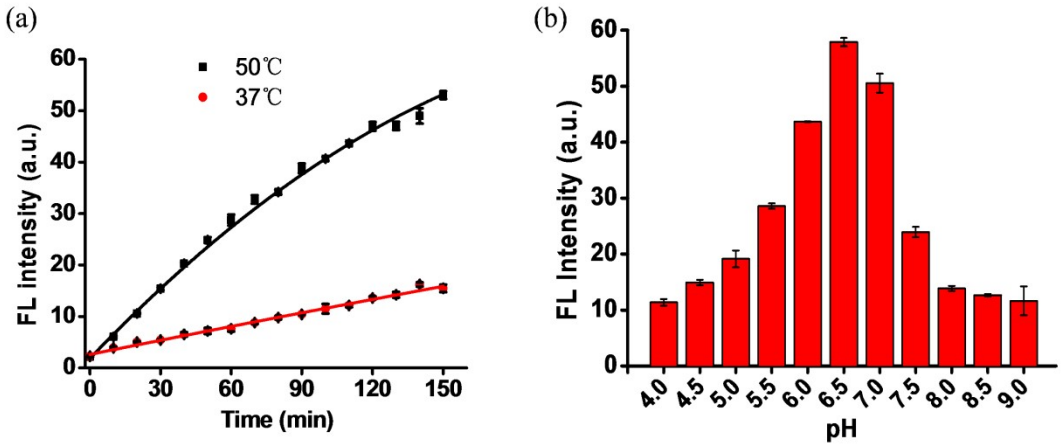

Fig.S1. (a) Kinetics study of P1-Cu^{2+} reaction under 37 °C and 50°C, PBS (pH 6.5) was used as the solvent. (b) Cu^{2+} detection under different pH conditions. The final concentration of P1 and Cu^{2+} were set at 100 μM and 20 μM respectively. λ_{ex} =390 nm, λ_{em} = 511nm.

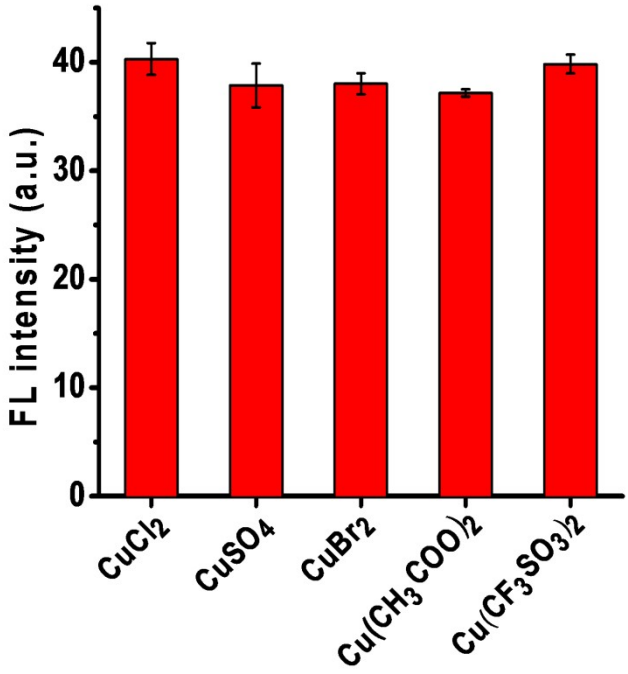

Fig.S2. Fluorescence detection of Cu^{2+} over different anions. Detection was performed in PBS (pH 6.5), the final concentration of P1 and copper salt were set at 100 μM and 2μM, respectively.

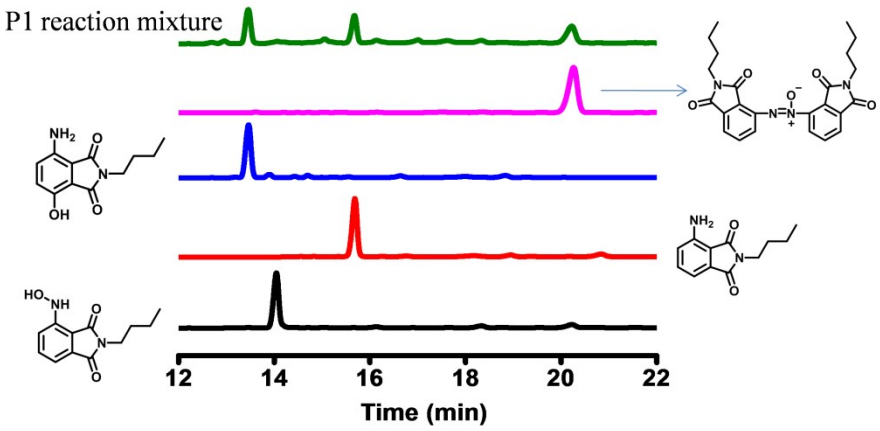

Fig. S3. HPLC analysis of the reaction solution of P1 (100 μM) and Cu^{2+} (100 μM). The reaction was performed at 50 °C until P1 was completely consumed. The traces were monitored by the absorbance at 254 nm.

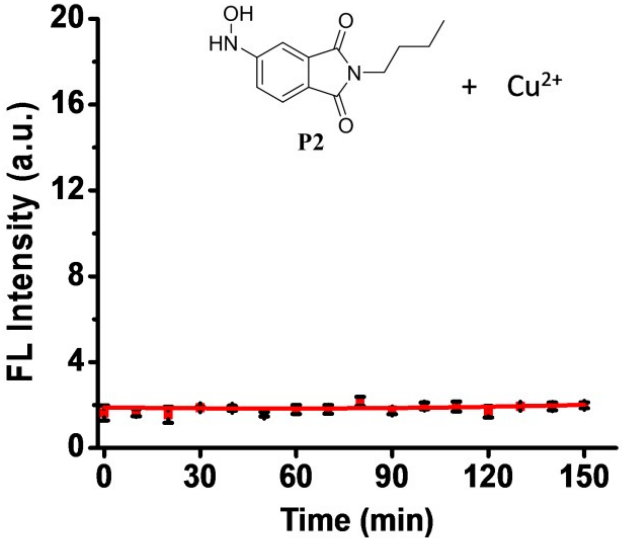

Fig. S4. Kinetic study of the fluorescence intensity from P2-Cu^{2+} solution over the reaction time. λ_{ex} =380 nm, λ_{em} = 525 nm. The concentration of P2 and Cu^{2+} were set at 100 μM and 20 μM, respectively.

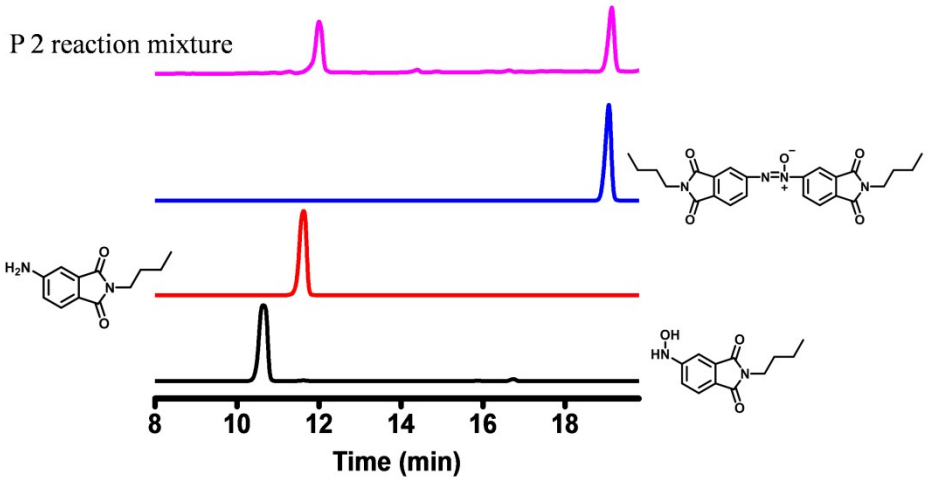

Fig. S5. HPLC analysis of the reaction solution of P2 (100 μM) and Cu^{2+} (100 μM). The reaction was performed at 50 °C until P2 was completely consumed. The traces were monitored by the absorbance at 254 nm.

HPLC analysis uses H_2O (mobile phase component A) mixed with ACN (mobile phase component B) as eluent following the sequence (A/B) 70:30 for 3 min, 70:30 to 20:80 during 8 min, 20:80 for 6 min, 20:80 to 70:30 during 3 min and then 70:30 for 3 min for P1; (A/B）60:40 for 2 min, 60:40 to 10:90 during 10 min, 10:90 for 3 min, 10:90 to 60:40 during 3 min and 60:40 for 2 min for P2.

4.3. The attempts to understand the rearrangement mechanism

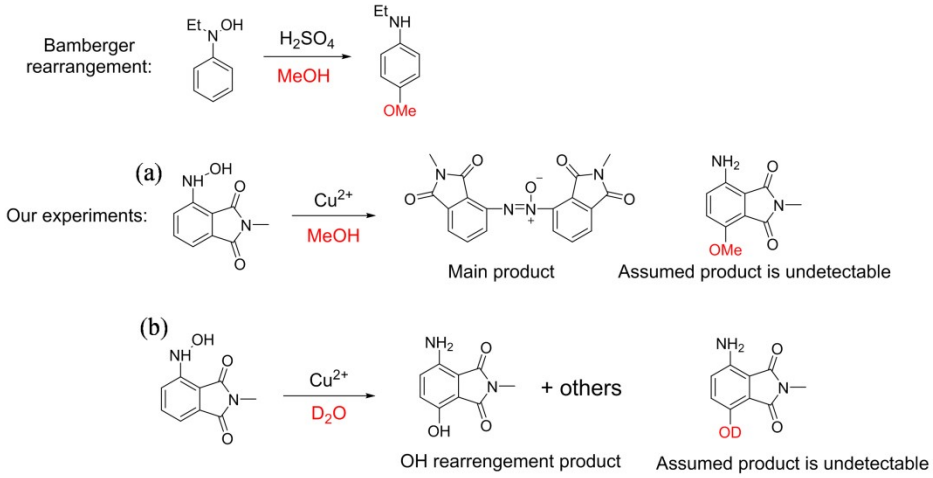

Scheme S1. Bamberger rearrangement reaction using methanol as the solvent and the reaction of 4c in the presence of Cu^{2+} using methanol and D_2O as the solvents, respectively.

We have put effort into the mechanism study and found some useful information, but it is still far from the fully understanding of the rearrangement mechanism. We noticed another reaction “Bamberger rearrangement” that can provide similar para-aminophenols from

hydroxylamines, which was usually performed in strong acidic mediums (e.g. sulfuric acid solution). Bamberger rearrangement is an intermolecular rearrangement, where the OH group is from H_2O of the aqueous solvent. This intermolecular rearrangement can be proved by performing the reaction using MeOH as the solvent, in which *p*-amino anisole formed as the major products.[13]

Answering it is an intermolecular or intramolecular rearrangement is critical for us to understand the mechanism. With this purpose, Cu^{2+} catalyzed reaction was performed in MeOH. However, no assumed rearranged products formed, and the azoxy product formed as the major product (Scheme S1a). In another experiment, the reaction was performed in D_2O buffer (phosphate and NaCl were dissolved in D_2O to prepared the PBS D_2O solution). The reaction mixture was examined by high-resolution mass spectrometry, however, there is no any OD substituted product formed (Scheme S1B).

We failed to obtain the direct evidence to support either intermolecular or intramolecular rearrangement mechanisms. Therefore, it is too hard for us to propose a reliable reaction mechanism at current stage. Doubtlessly, great efforts have to be put in.

4.4 Fluorescence lifetime measurement

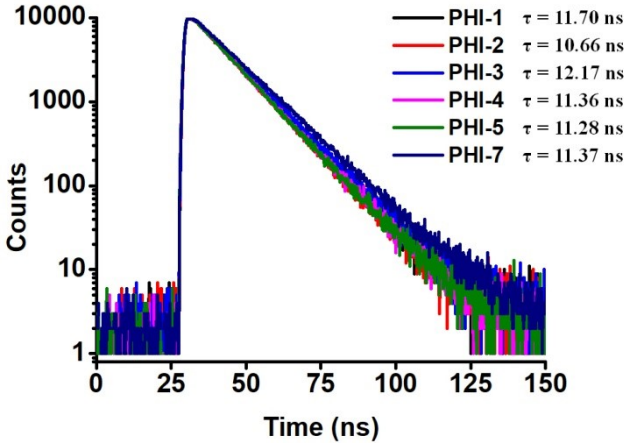

Fig. S6. Fluorescence lifetimes (τ) of the newly synthesized PHI-3, PHI-4, PHI-5 and PHI-7 versus PHI-1 and PHI-2.

The data was measured using PBS 7.4 solution containing each dye at 20 μM. The average fluorescence lifetime was calculated from the double fit exponential function.[14]

4.5 The spectrum characterization

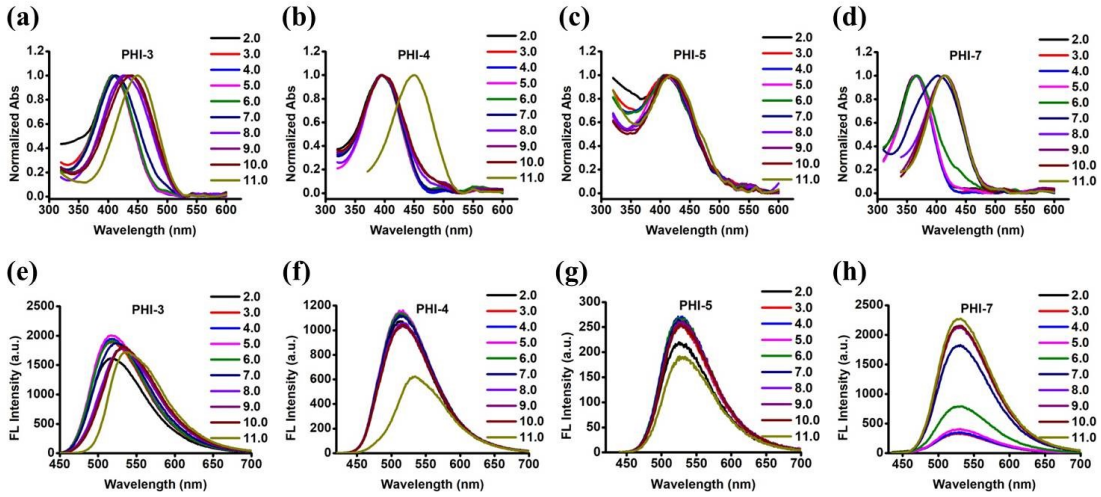

Fig. S7. The spectrum characterization of PHI-3, PHI-4, PHI-5 and PHI-7 in PBS buffer with different pH values (pH 2.0- pH 11.0). (a-d) the UV-vis absorbance spectra, (e-h) the fluorescence spectra. The value of maximum absorbance was normalized to 1 for easy comparison.

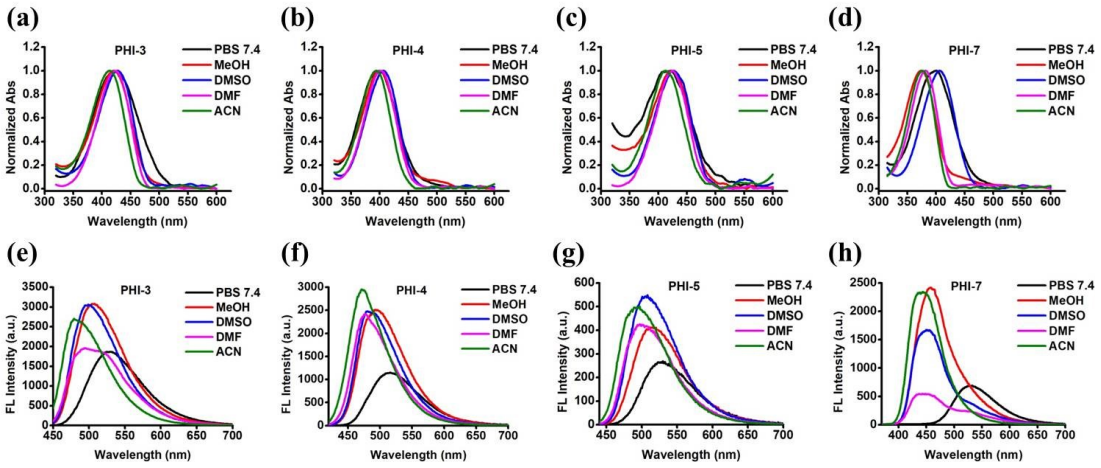

Fig. S8. The spectrum characterization of PHI-3, PHI-4, PHI-5 and PHI-7 in different solvent systems (PBS 7.4, methanol, dimethyl sulfoxide, dimethylformamide and acetonitrile) . (a-d) the absorbance spectra, (e-h) the fluorescence spectra. The value of maximum absorbance was normalized to 1 for easy comparison.

The final concentrations of PHI-3, PHI-4 and PHI-7 were set at 20 μM except PHI-5 (60 μM).

4.6 Green fluorescent molecules

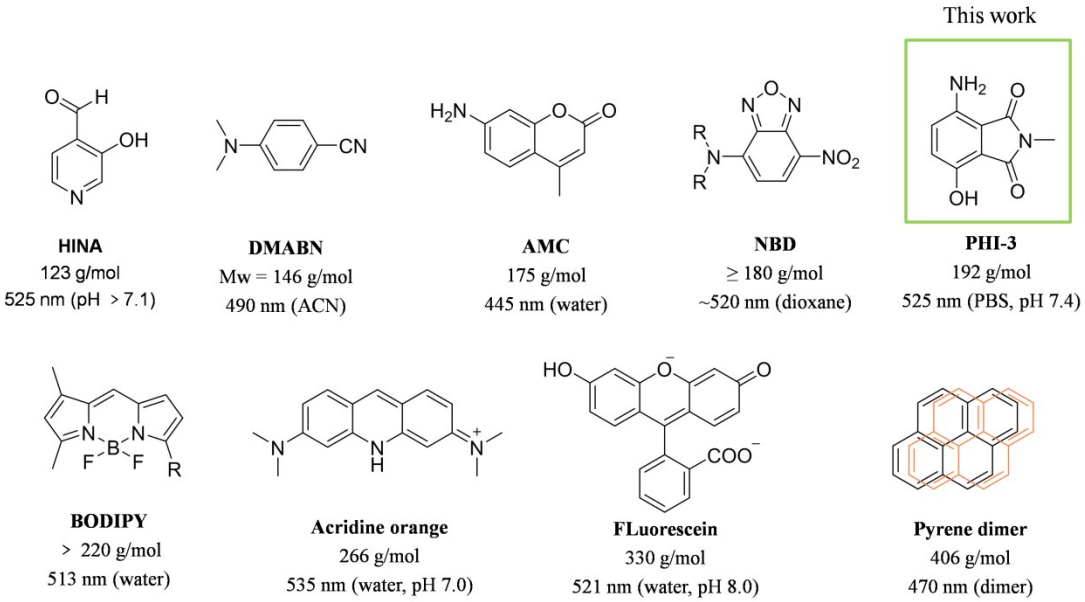

Fig. S9. The structures of dyes with typical green fluorescence or blue-green fluorescence. The contents were modified and renewed from the literature *Chem. Sci*.,2021, 12,1392.

5. HPLC and NMR spectra

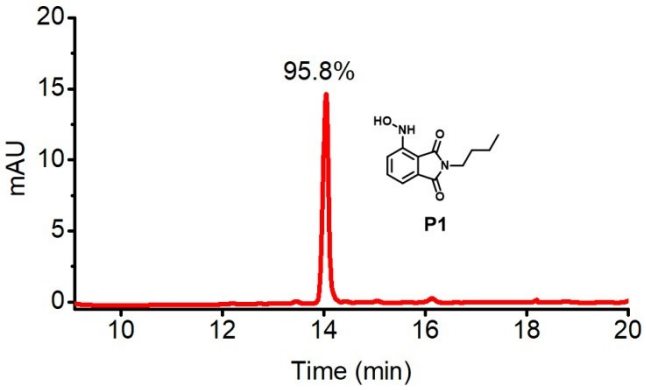

Fig. S10. HPLC analysis of P1, the purity reaches to 95.8% according to the HPLC-DAD chromatograms at 254 nm.

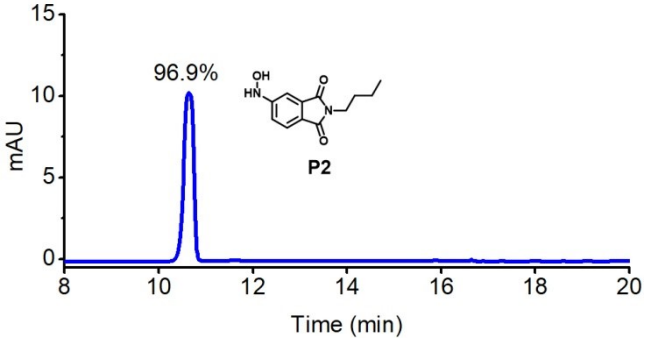

Fig. S11. HPLC analysis of P2, the purity of P2 reaches to 96.9% according to the HPLC-DAD chromatograms at 254 nm.

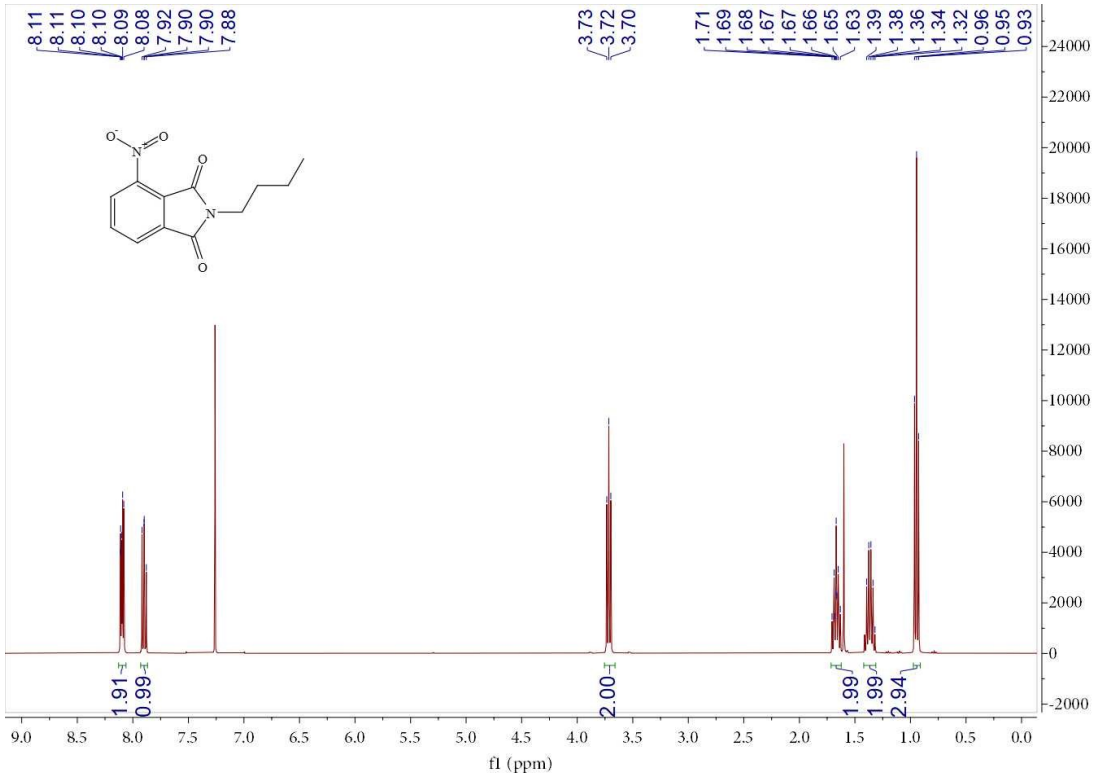

Fig.S12 ^{1}H NMR spectrum of compound **3a.**

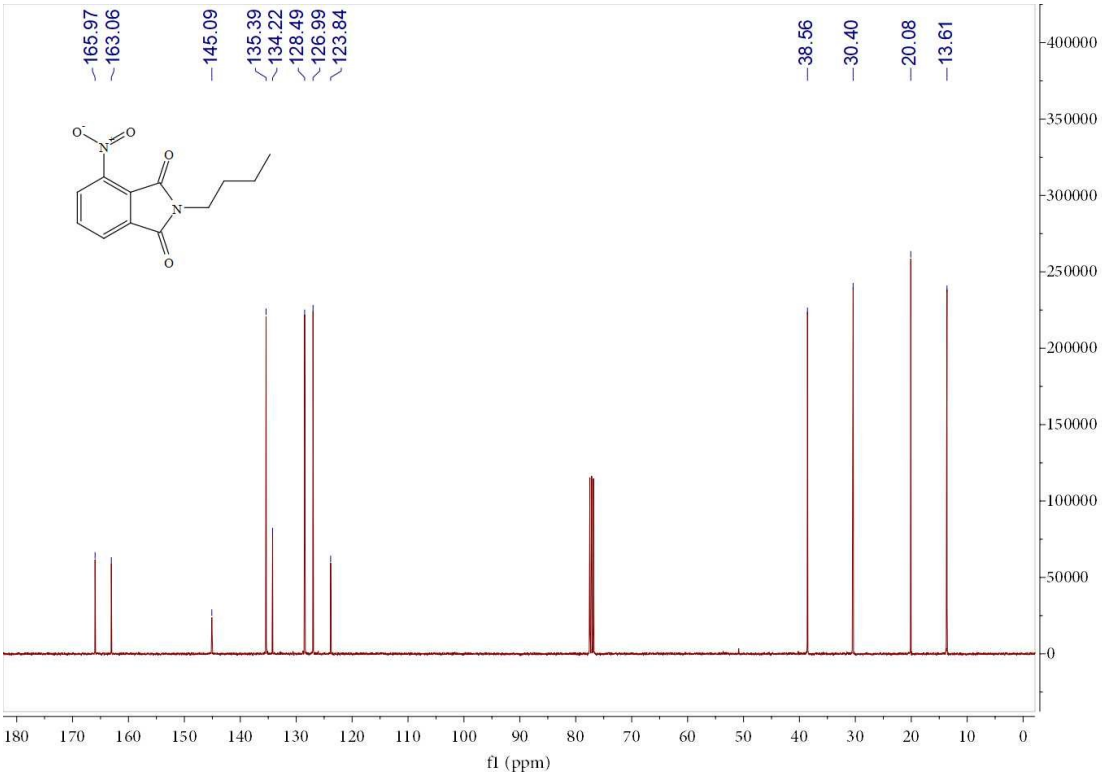

Fig.S13 ^{13}C NMR spectrum of compound **3a.**

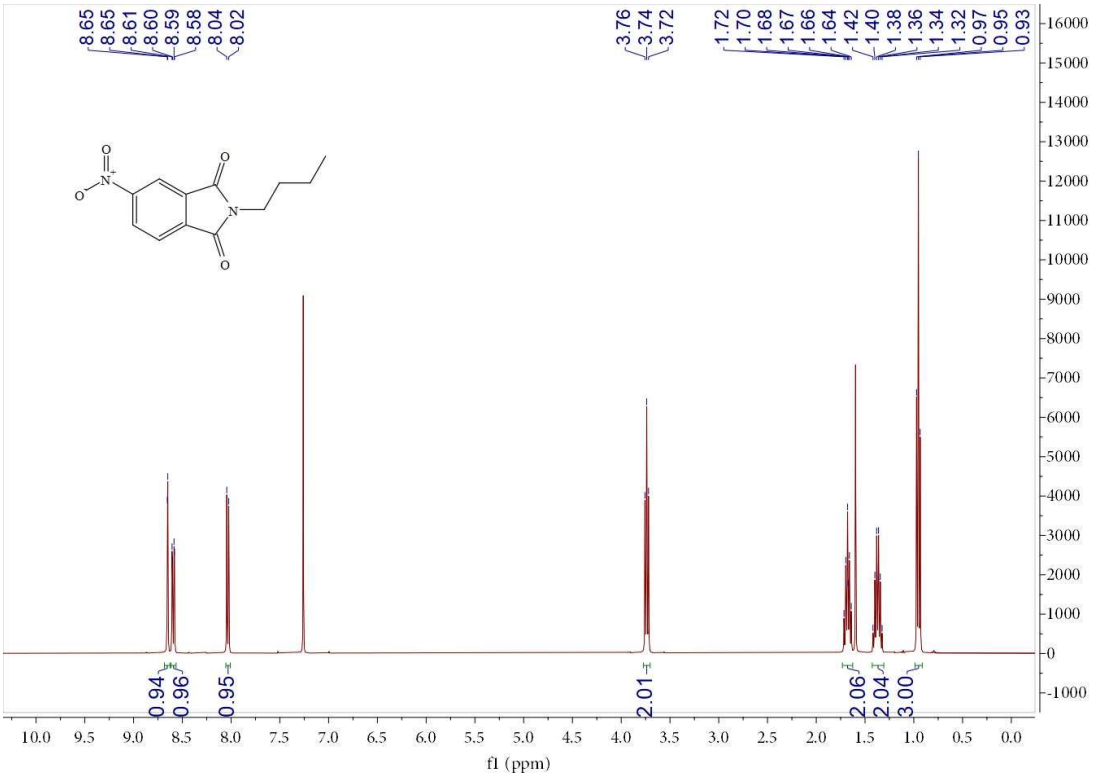

Fig.S14[1]H NMR spectrum of compound **3b.**

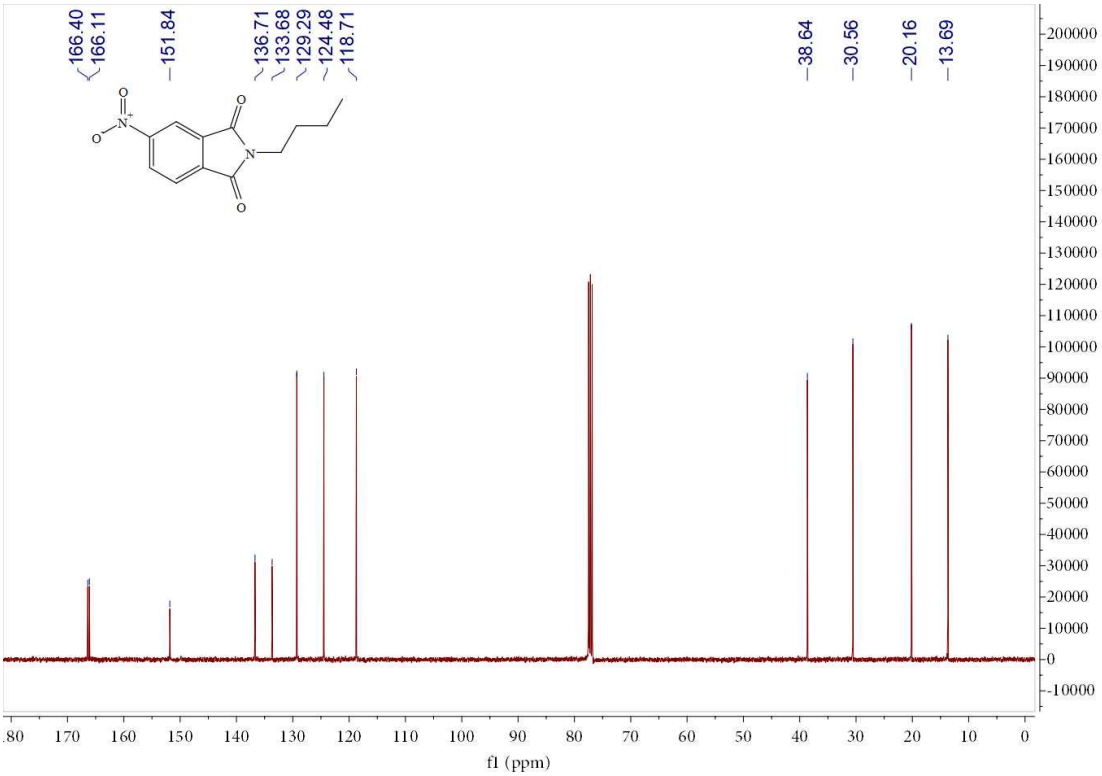

Fig.S15 [13]C NMR spectrum of compound **3b.**

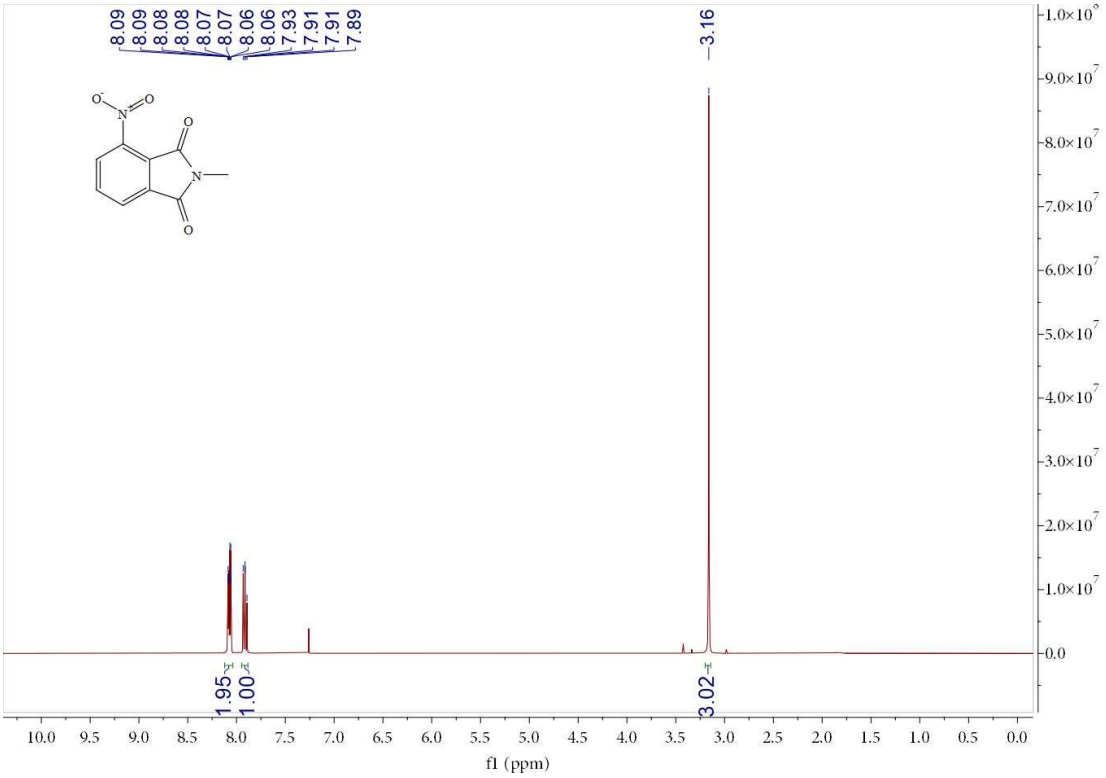

Fig.S16 ^{1}H NMR spectrum of compound **3c.**

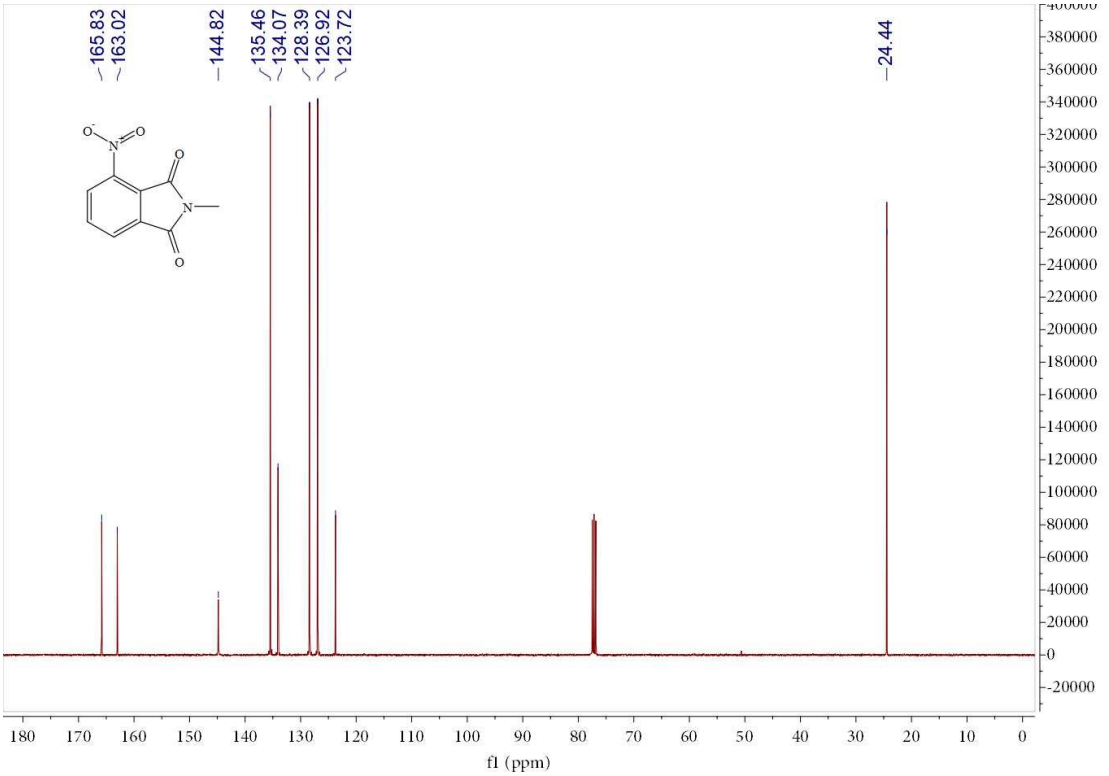

Fig.S17 ^{13}C NMR spectrum of compound **3c.**

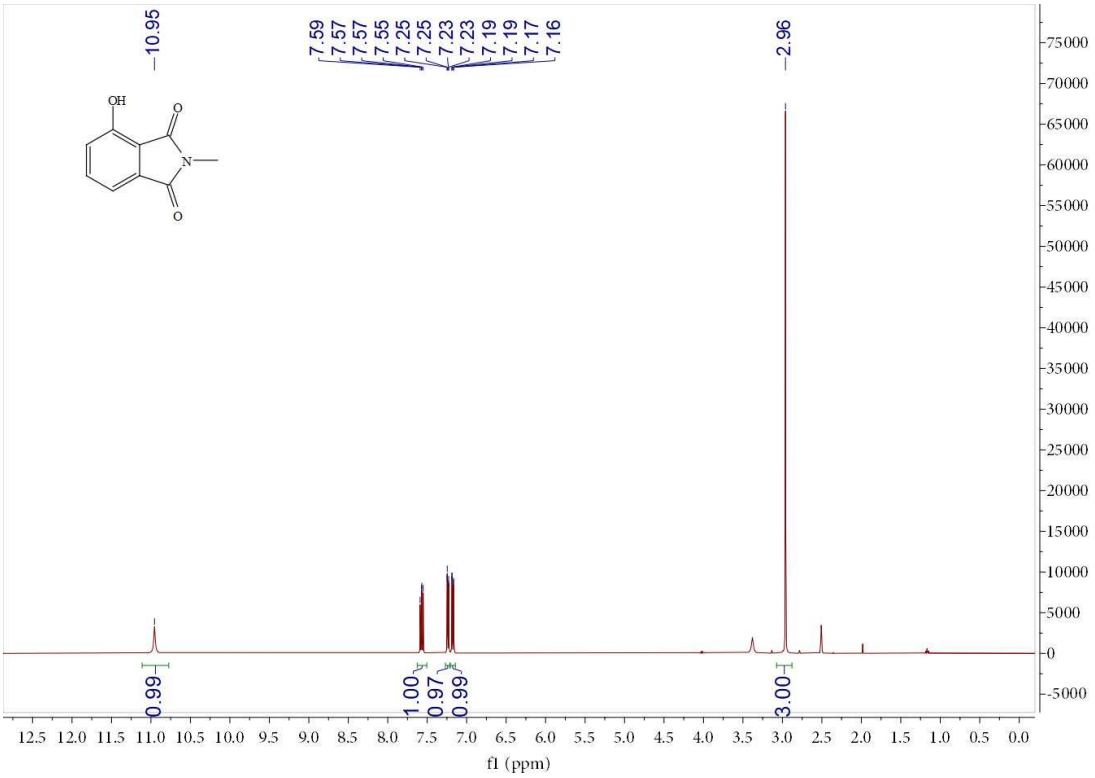

Fig.S18 ^{1}H NMR spectrum of compound **3d** (**PHI-1**).

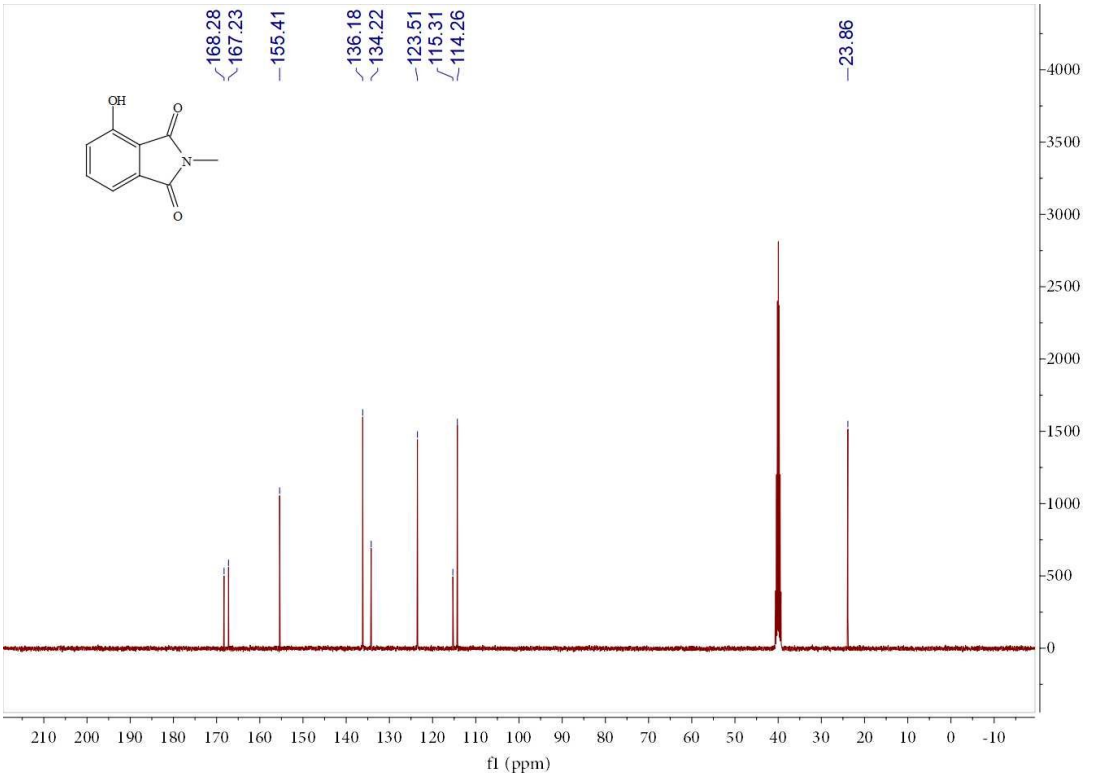

Fig.S19 ^{13}C NMR spectrum of compound **3d** (**PHI-1**).

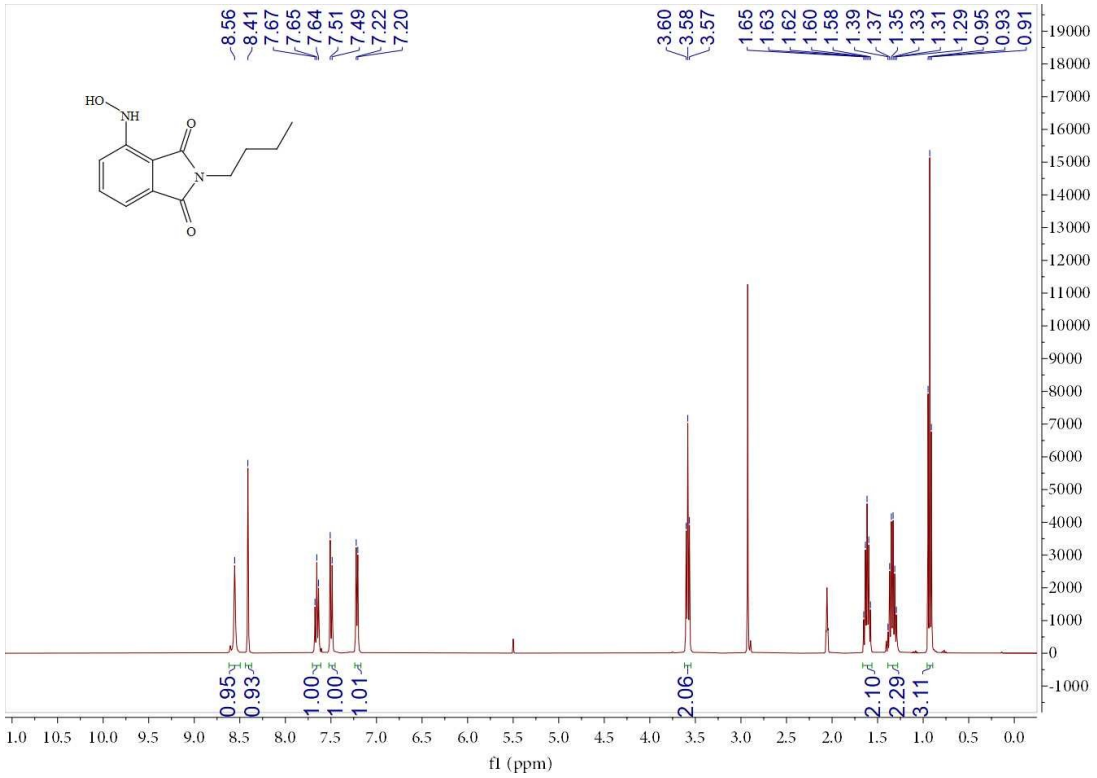

Fig.S20 ^{1}H NMR spectrum of compound **4a (P1).**

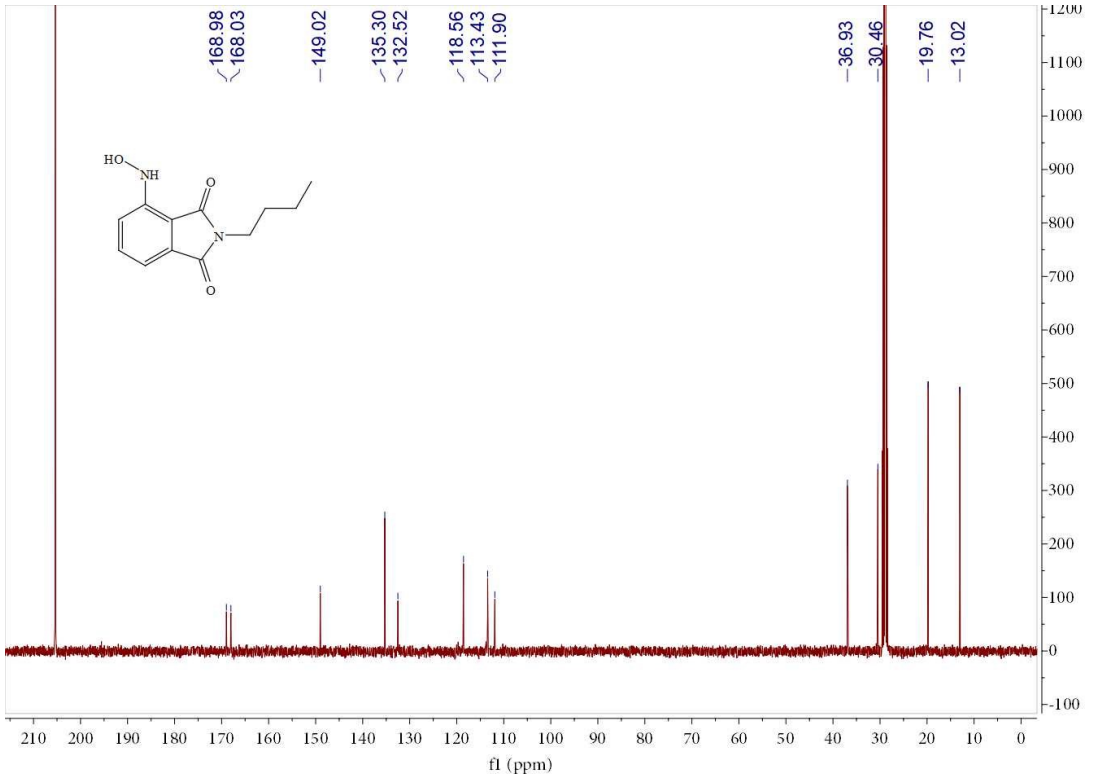

Fig.S21^{13}C NMR spectrum of compound **4a (P1).**

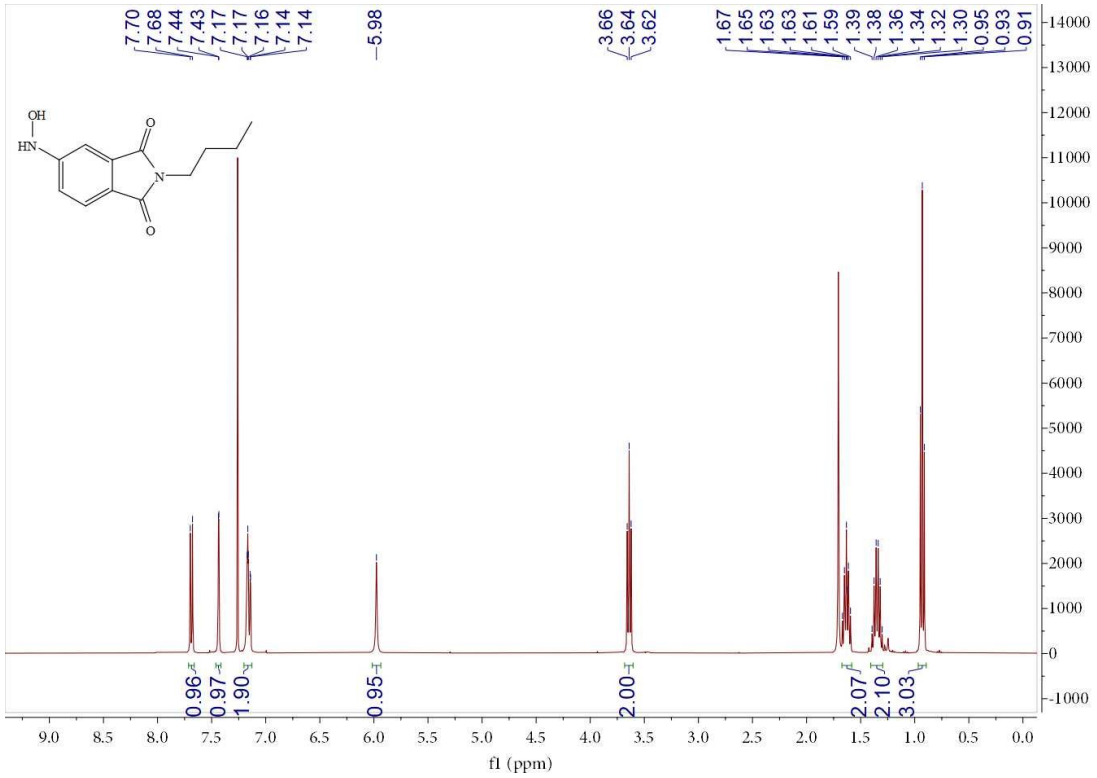

Fig.S22 [1]H NMR spectrum of compound **4b (P2).**

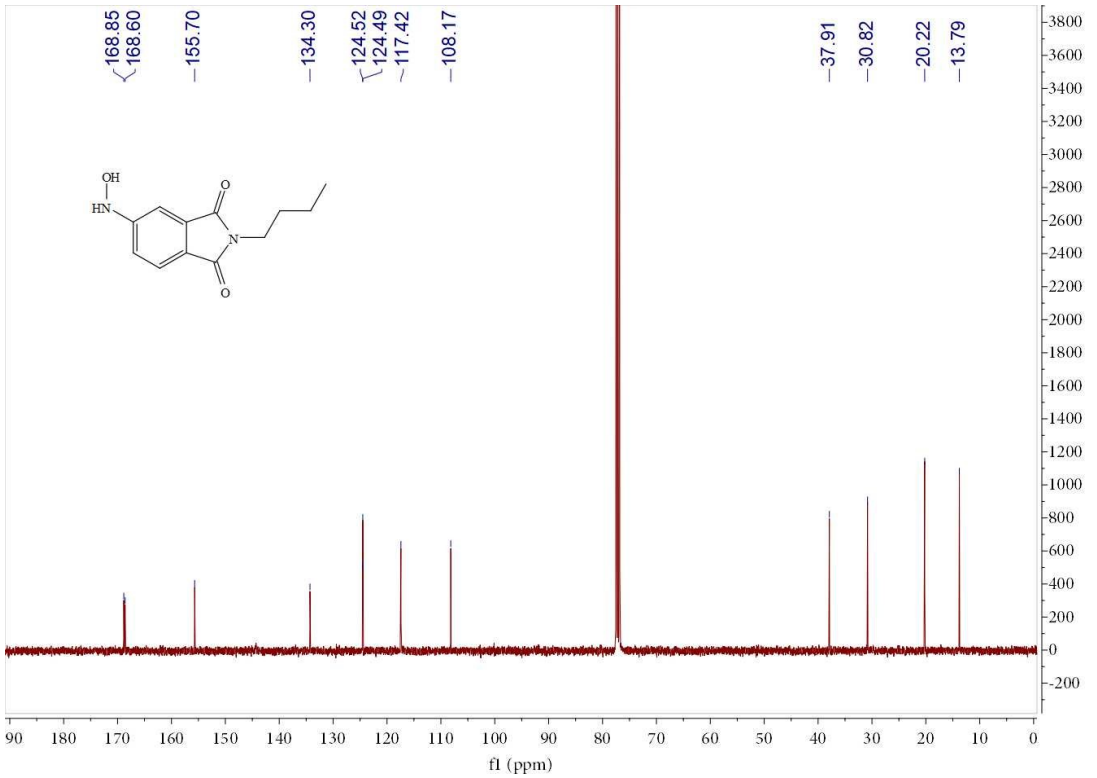

Fig.S23 [13]C NMR spectrum of compound **4b (P2).**

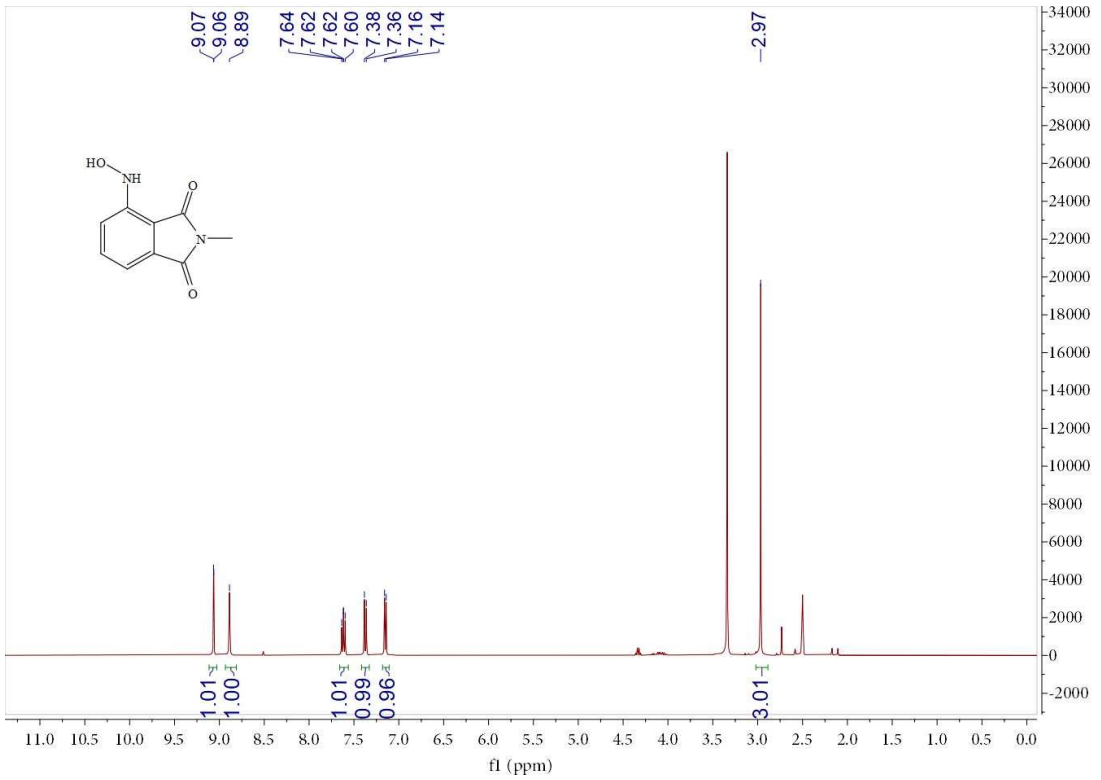

Fig.S24 [1]H NMR spectrum of compound **4c.**

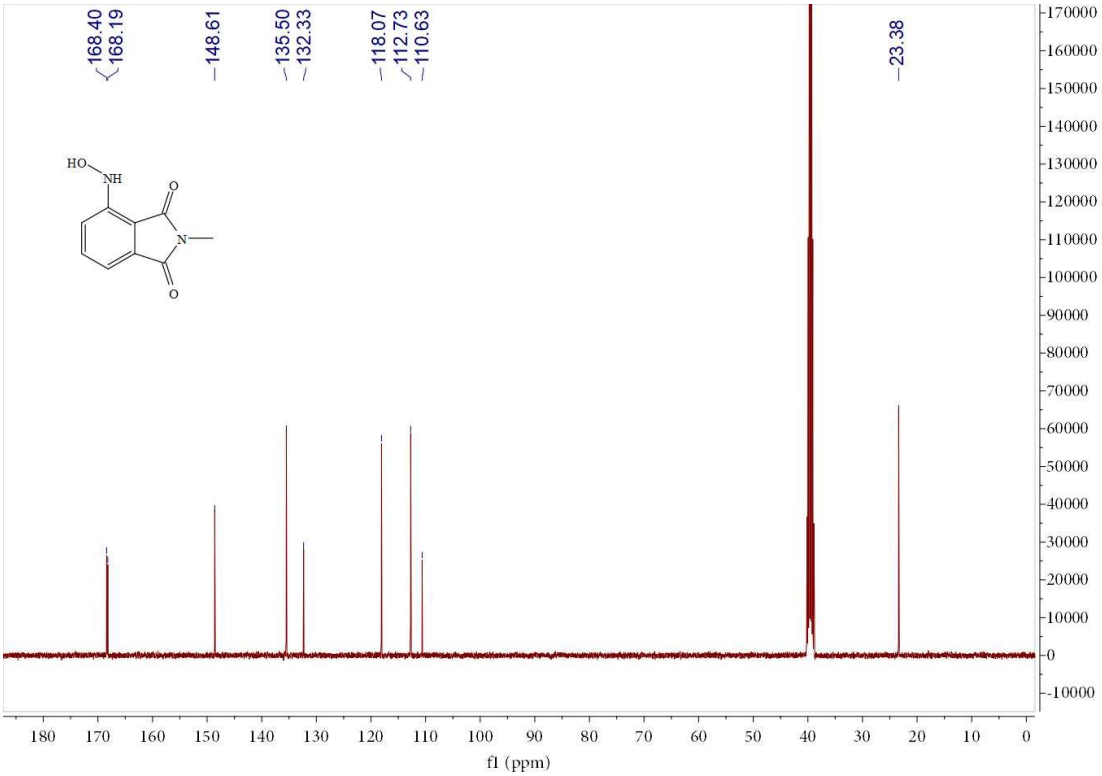

Fig.S25 [13]C NMR spectrum of compound **4c.**

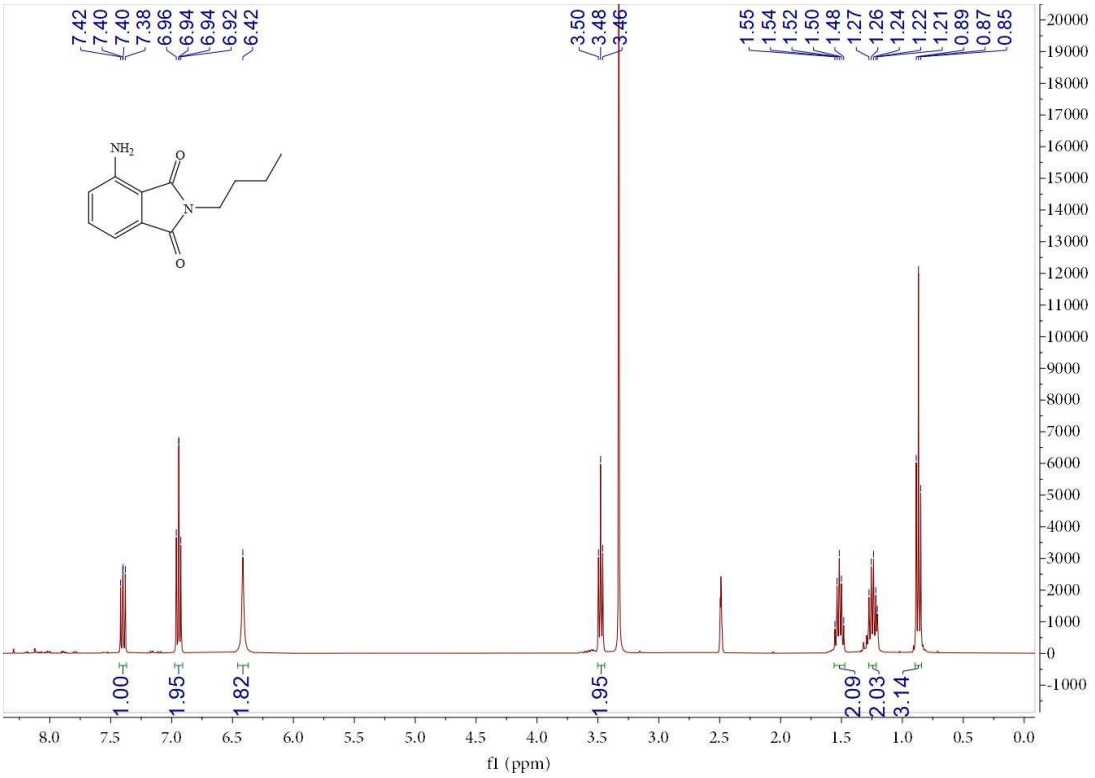

Fig.S26 ^{1}H NMR spectrum of compound **5a.**

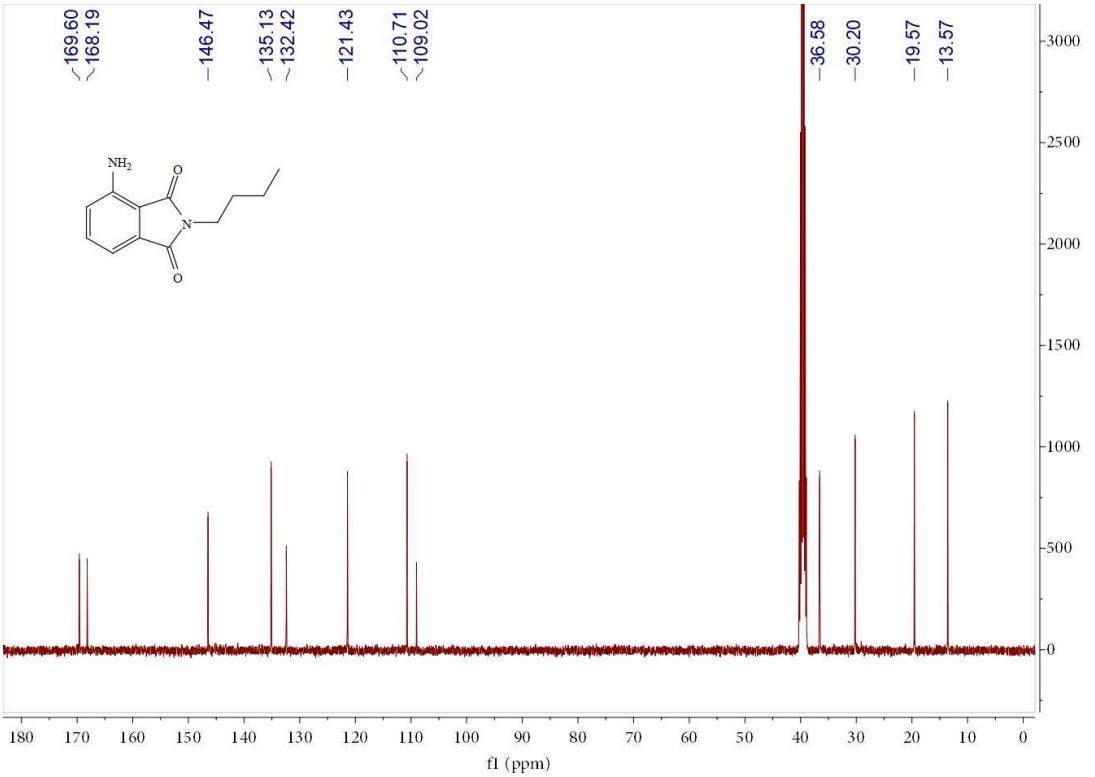

Fig.S27 ^{13}C NMR spectrum of compound **5a.**

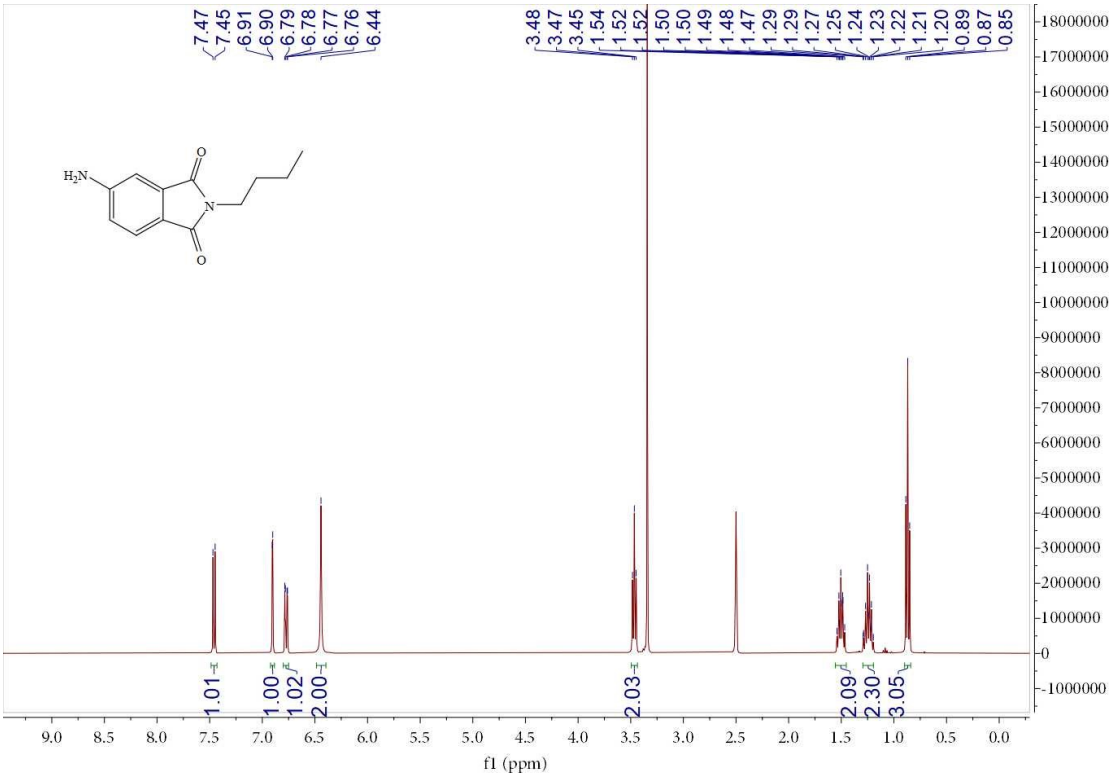

Fig.S28 [1]H NMR spectrum of compound **5b.**

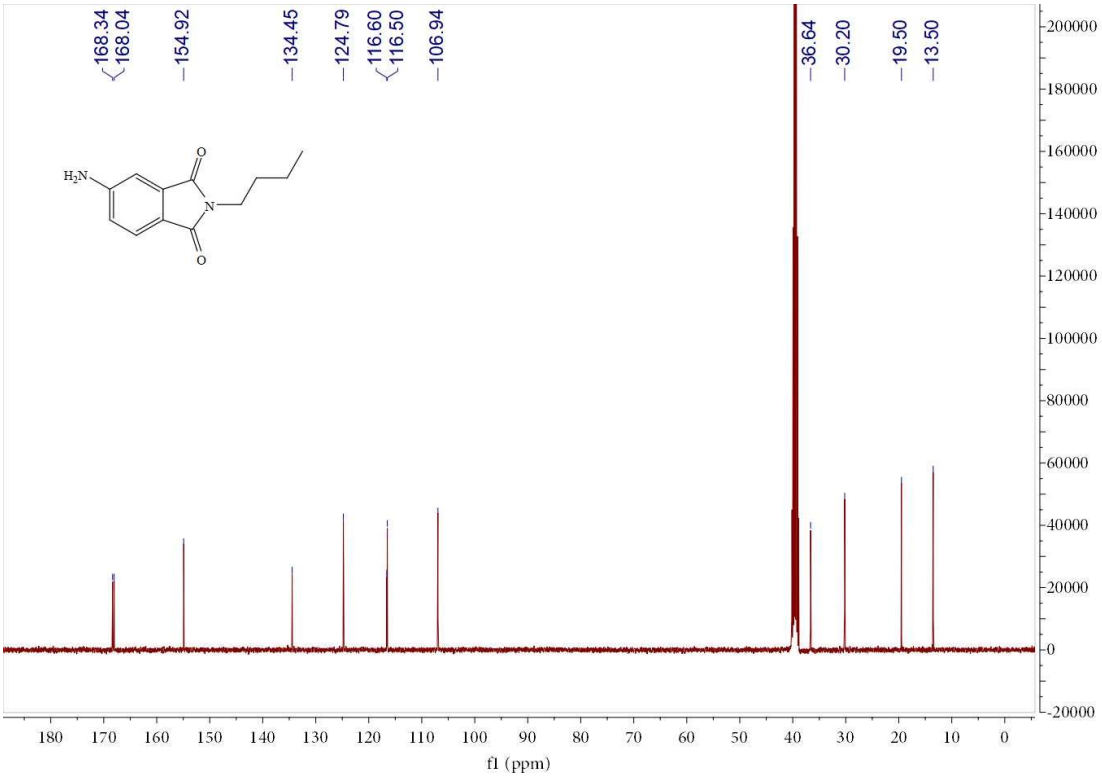

Fig.S29 [13]C NMR spectrum of compound **5b.**

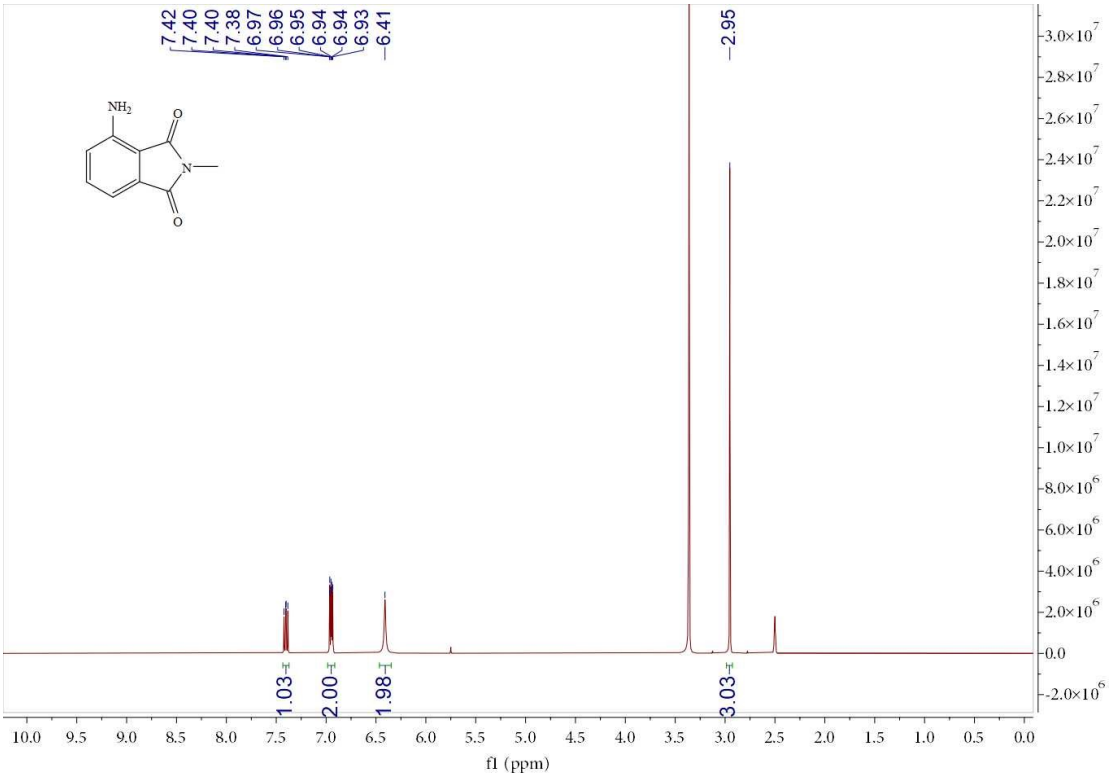

Fig.S30 ^{1}H NMR spectrum of compound **5c** (**PHI-2**).

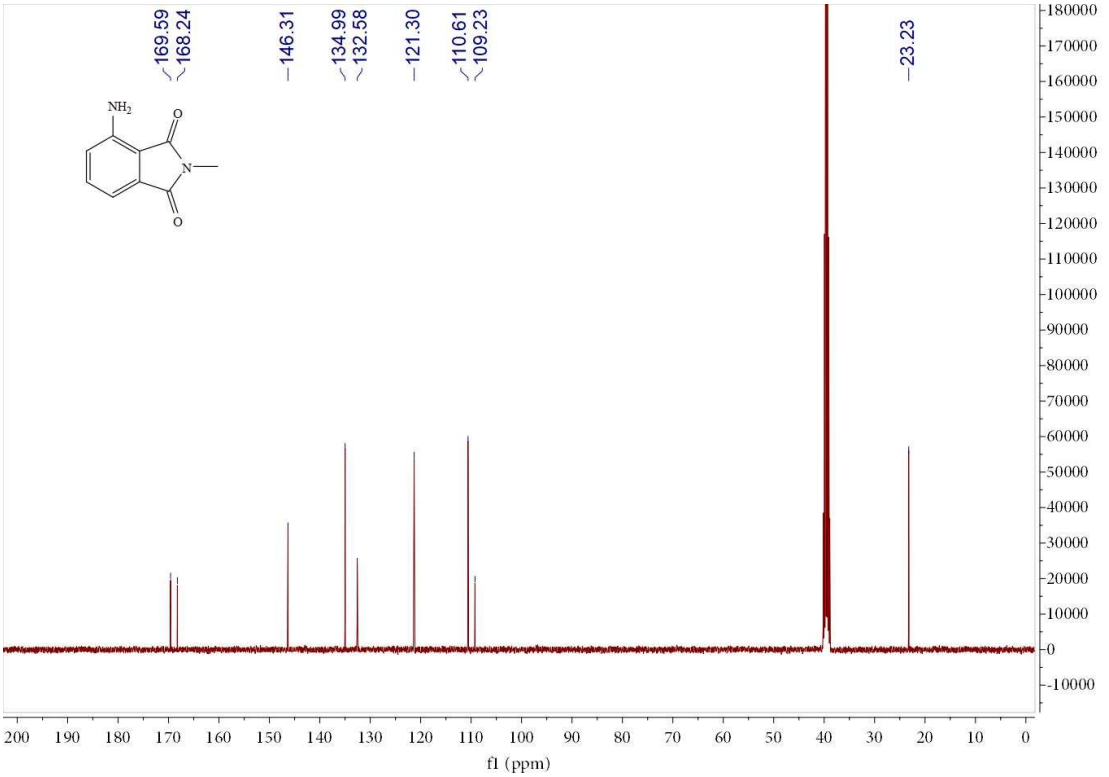

Fig.S31^{13}C NMR spectrum of compound **5c** (**PHI-2**).

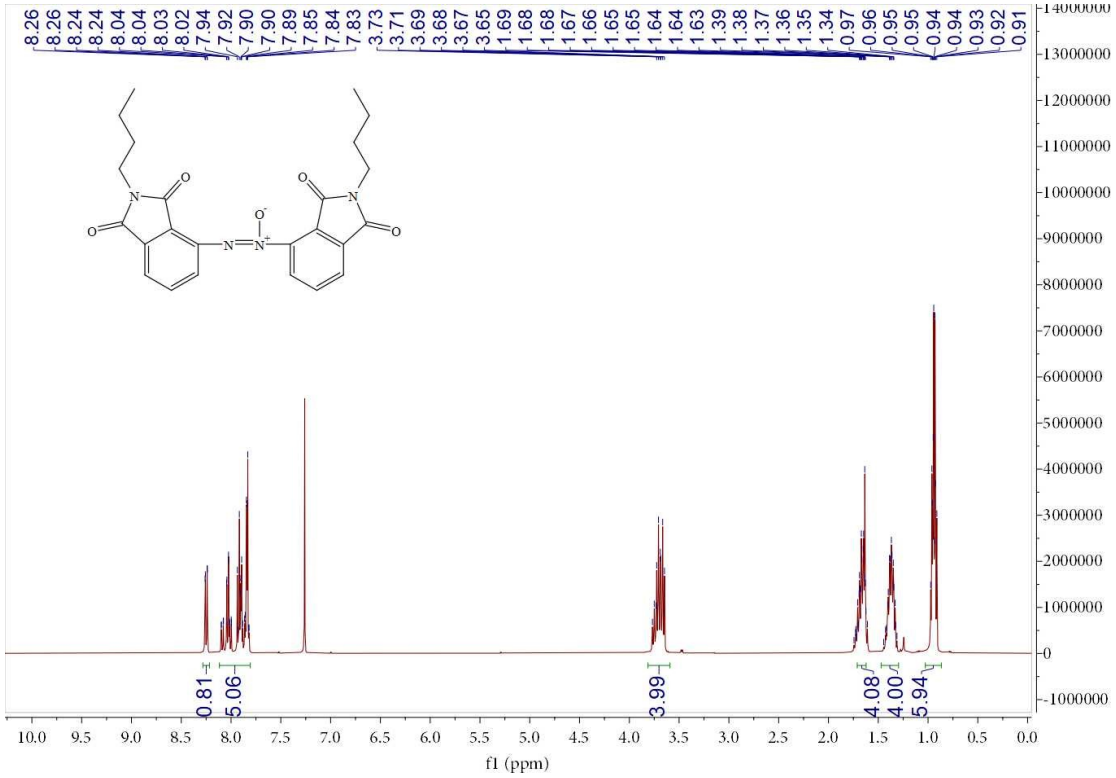

Fig.S32[1]H NMR spectrum of compound **6a.**

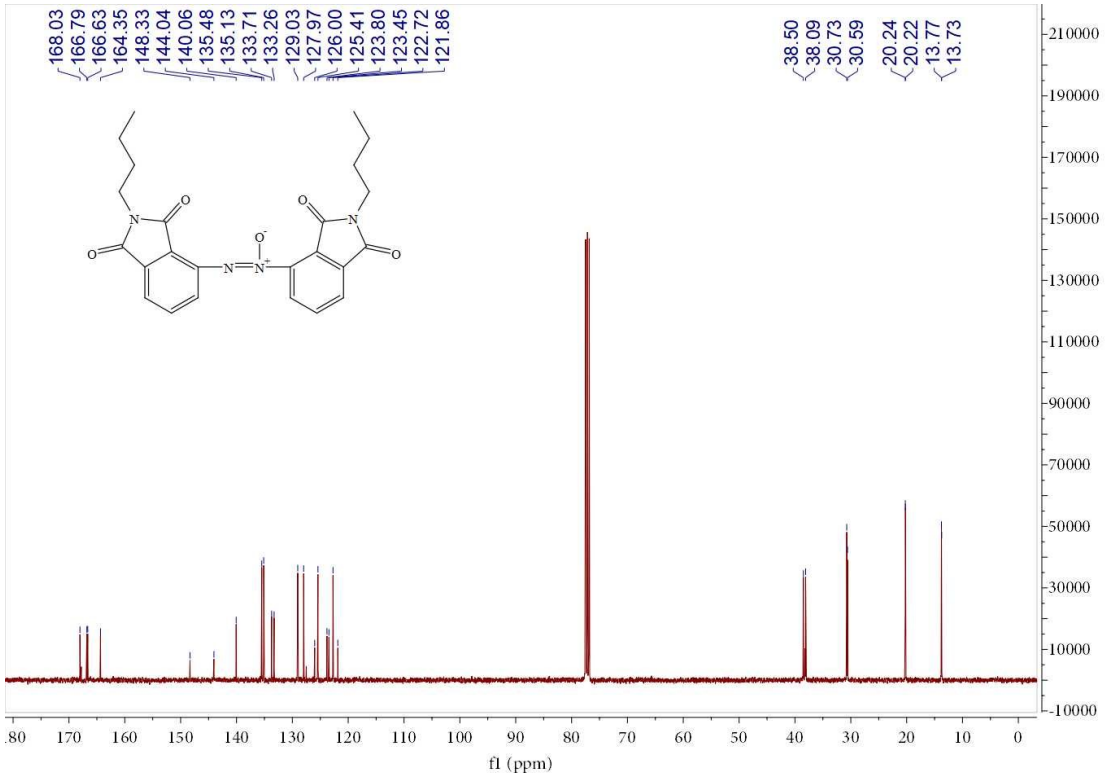

Fig.S33 [13]C NMR spectrum of compound **6a.**

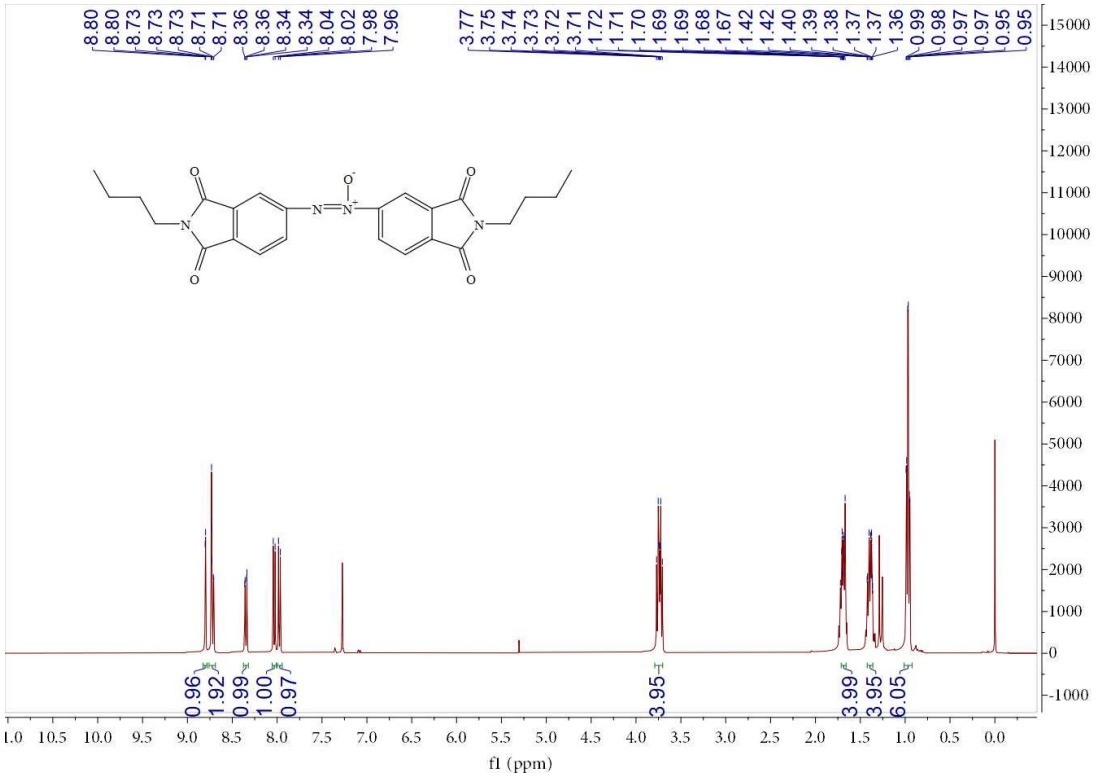

Fig.S34 ^{1}H NMR spectrum of compound **6b.**

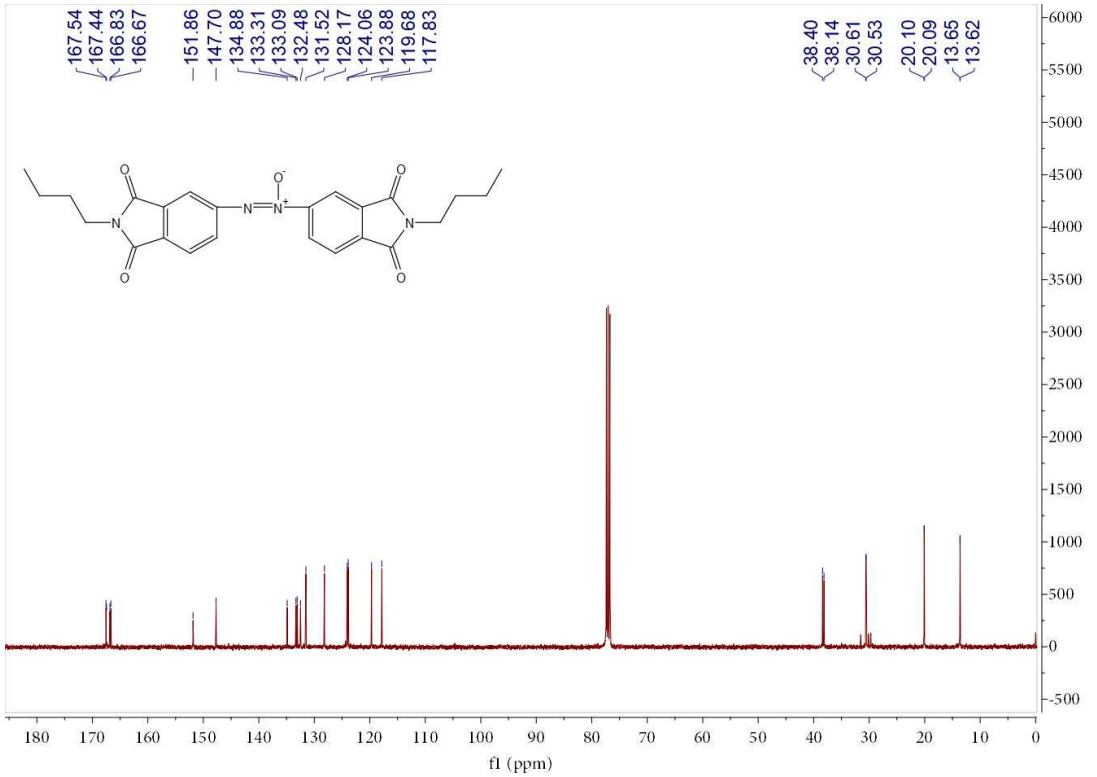

Fig.S35 ^{13}C NMR spectrum of compound **6b.**

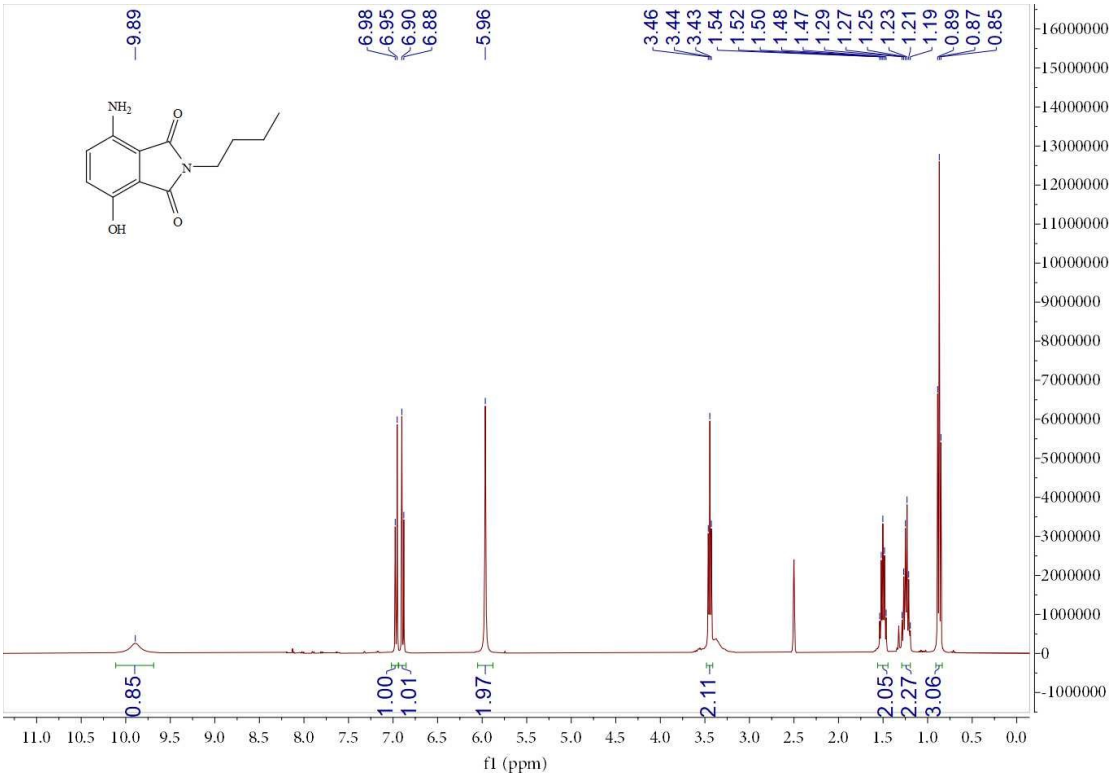

Fig.S36 ^{1}H NMR spectrum of compound **7a.**

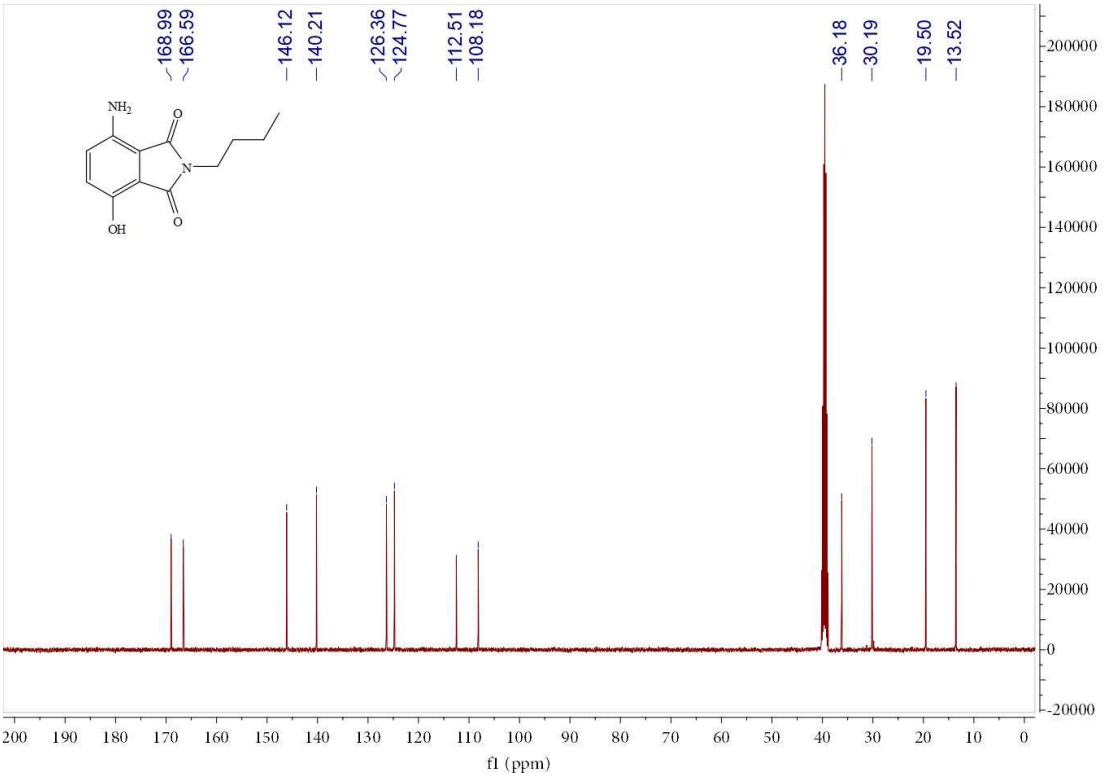

Fig.S37 ^{13}C NMR spectrum of compound **7a.**

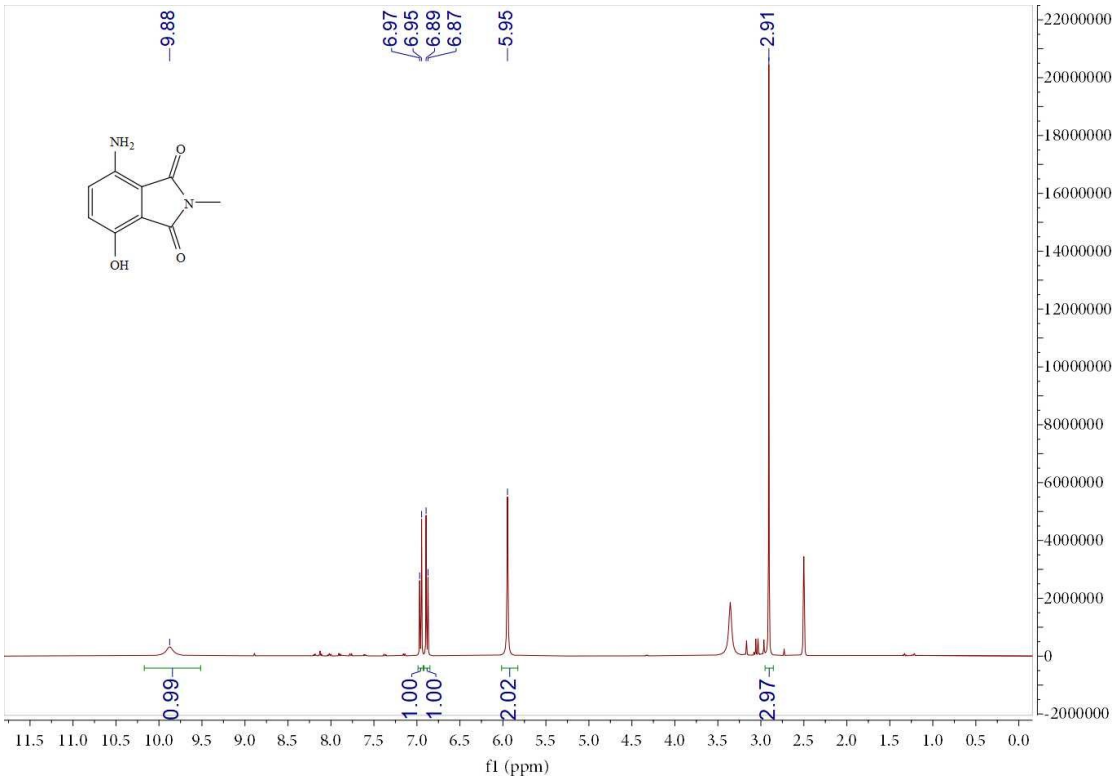

Fig.S38 ^{1}H NMR spectrum of compound **7b** (**PHI-3**).

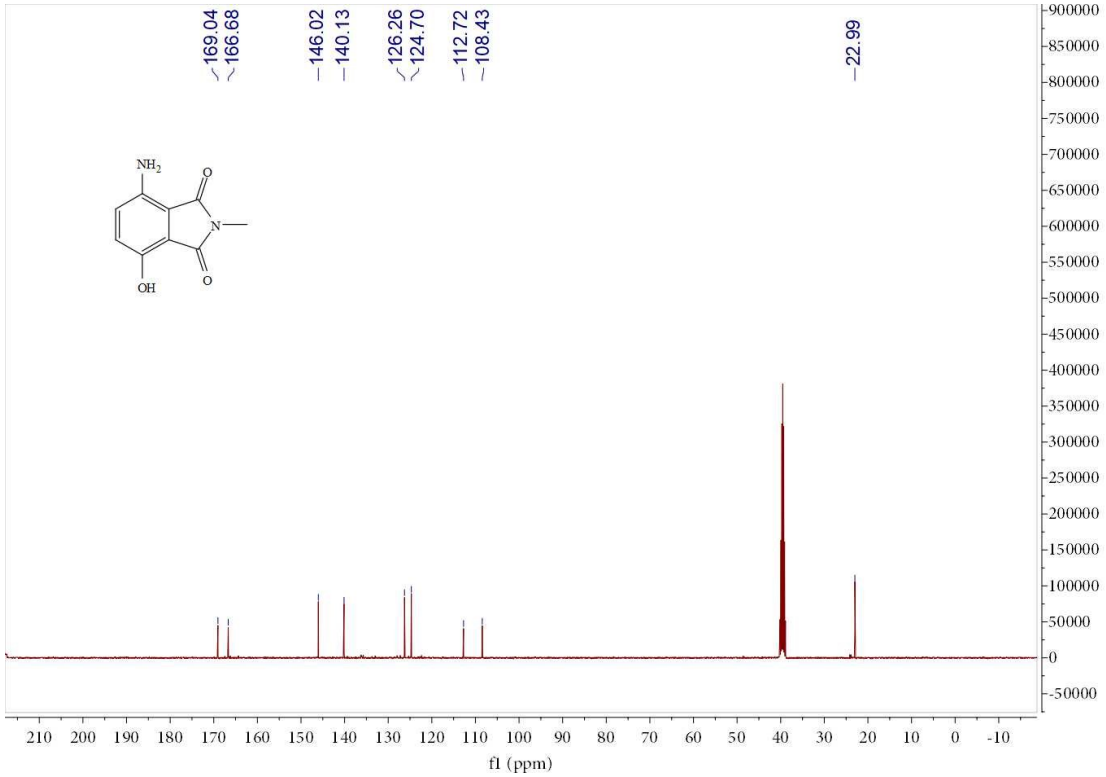

Fig.S39 ^{13}C NMR spectrum of compound **7b** (**PHI-3**).

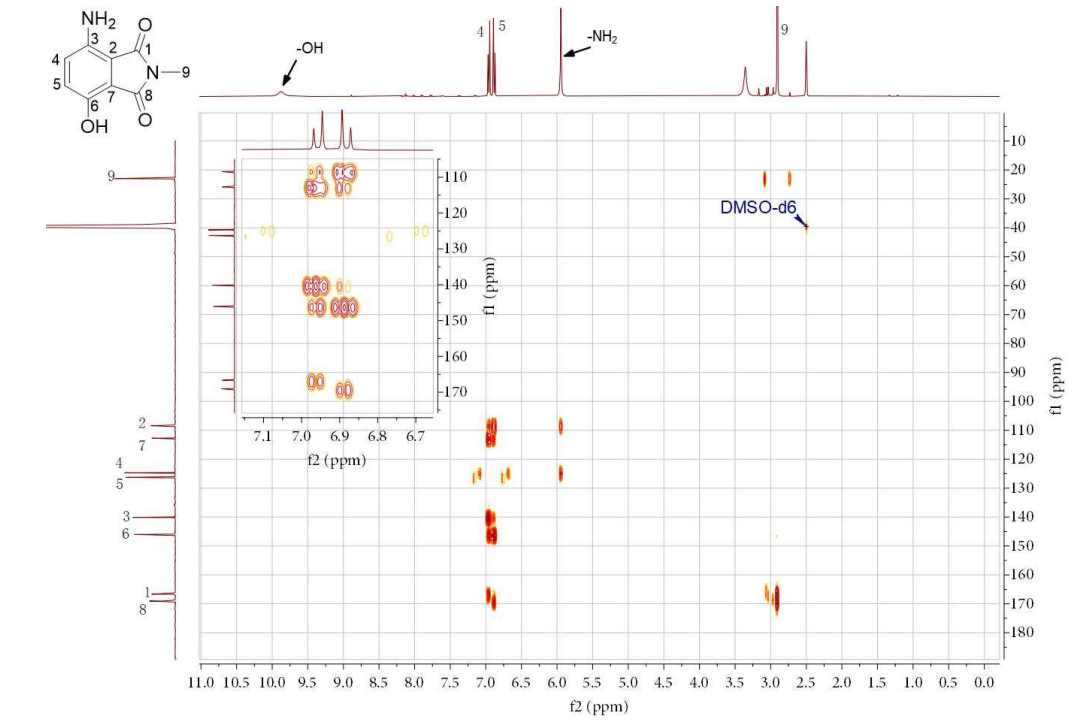

Fig. S40. HMBC spectrum of compound **7b (PHI-3)**.

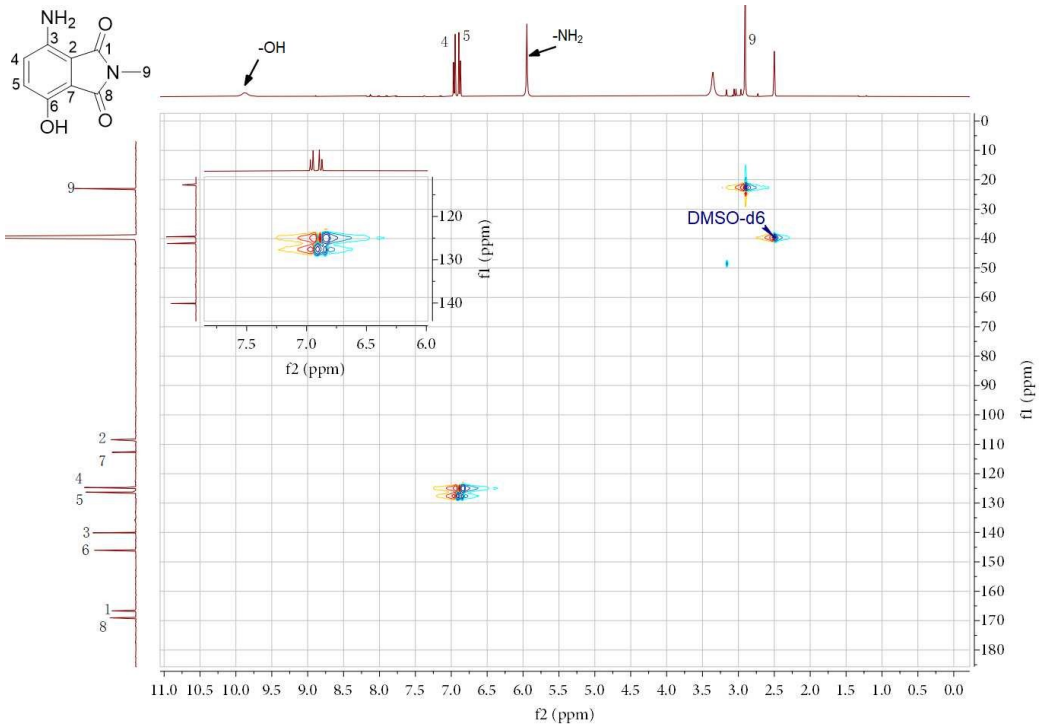

Fig. S41. HSQC spectrum of compound **7b (PHI-3).**

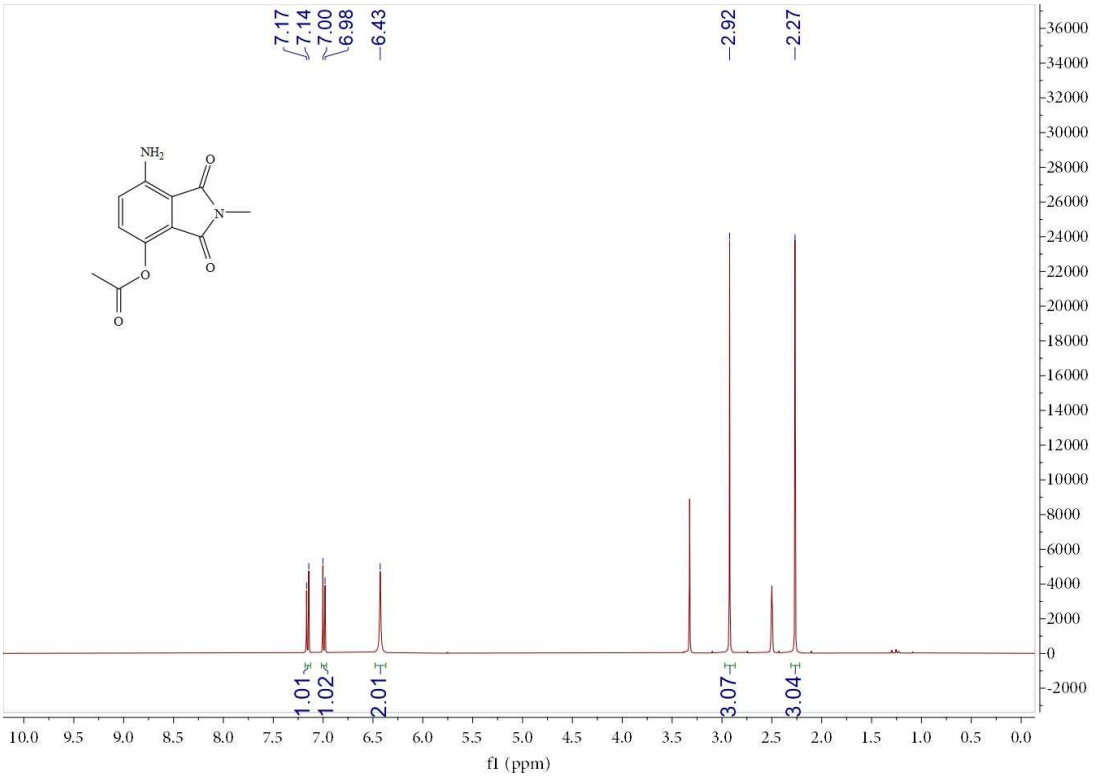

Fig.S42 ^{1}H NMR spectrum of compound **8a**(**PHI-4**).

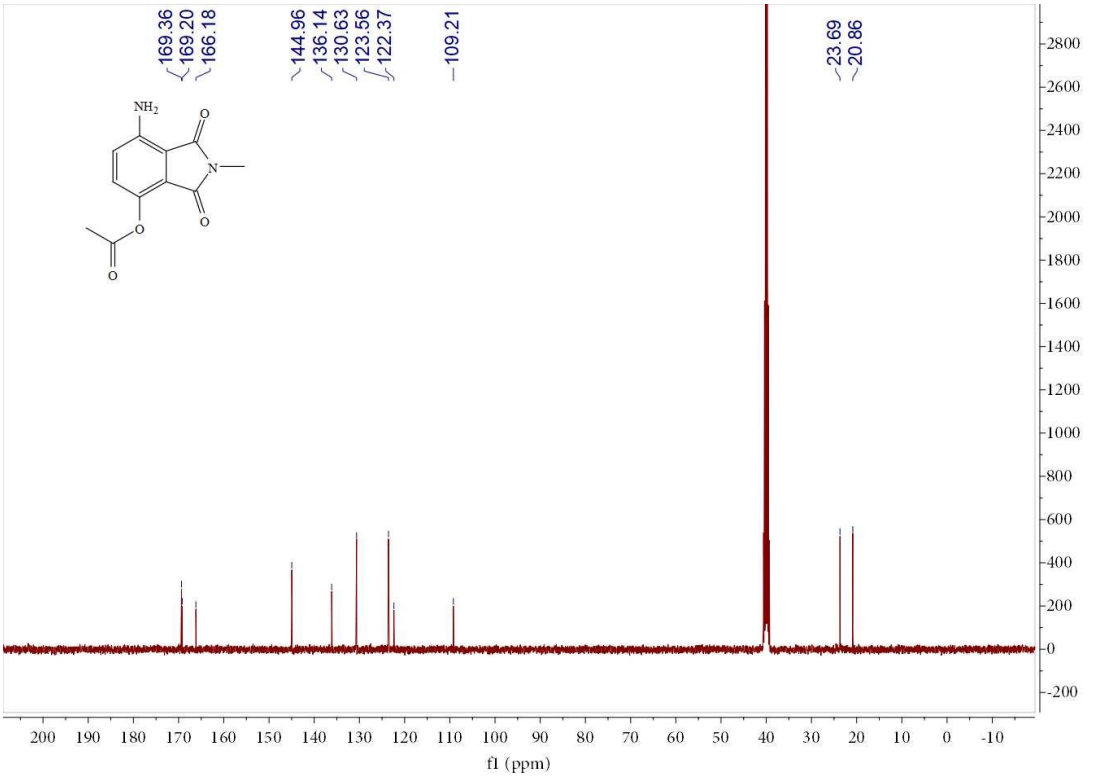

Fig.S43 ^{13}C NMR spectrum of compound **8a** (**PHI-4**).

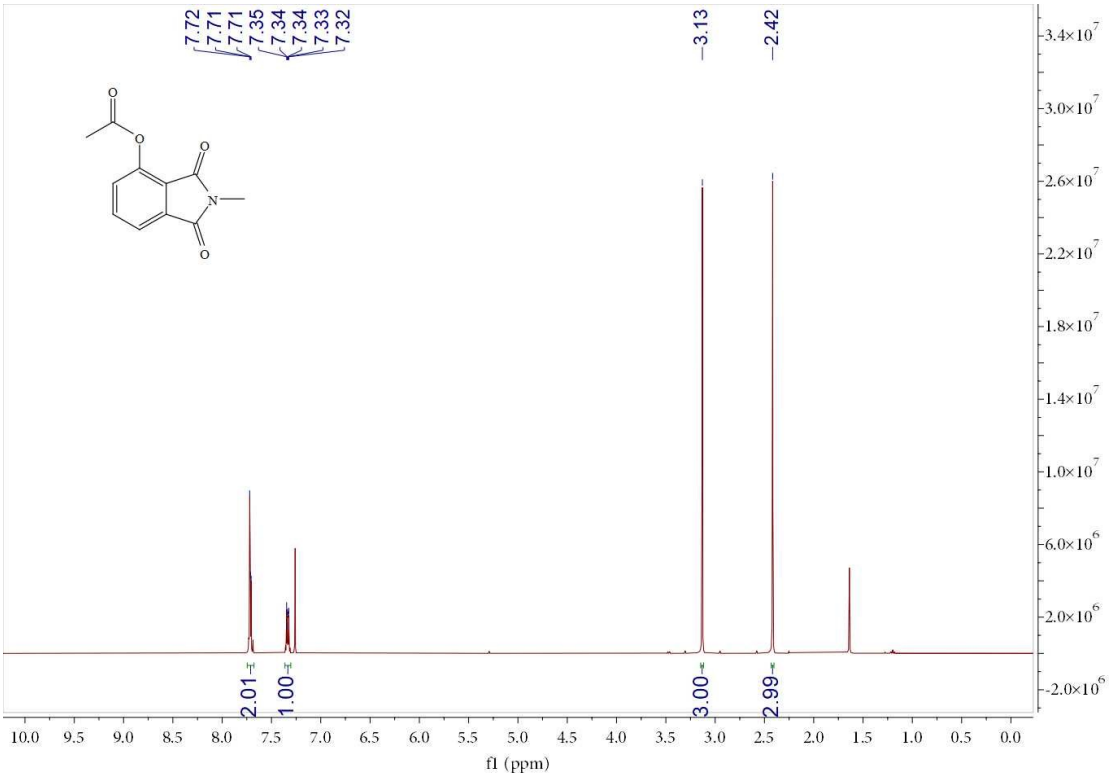

Fig.S44 ^{1}H NMR spectrum of compound **8b** (**PHI-6**).

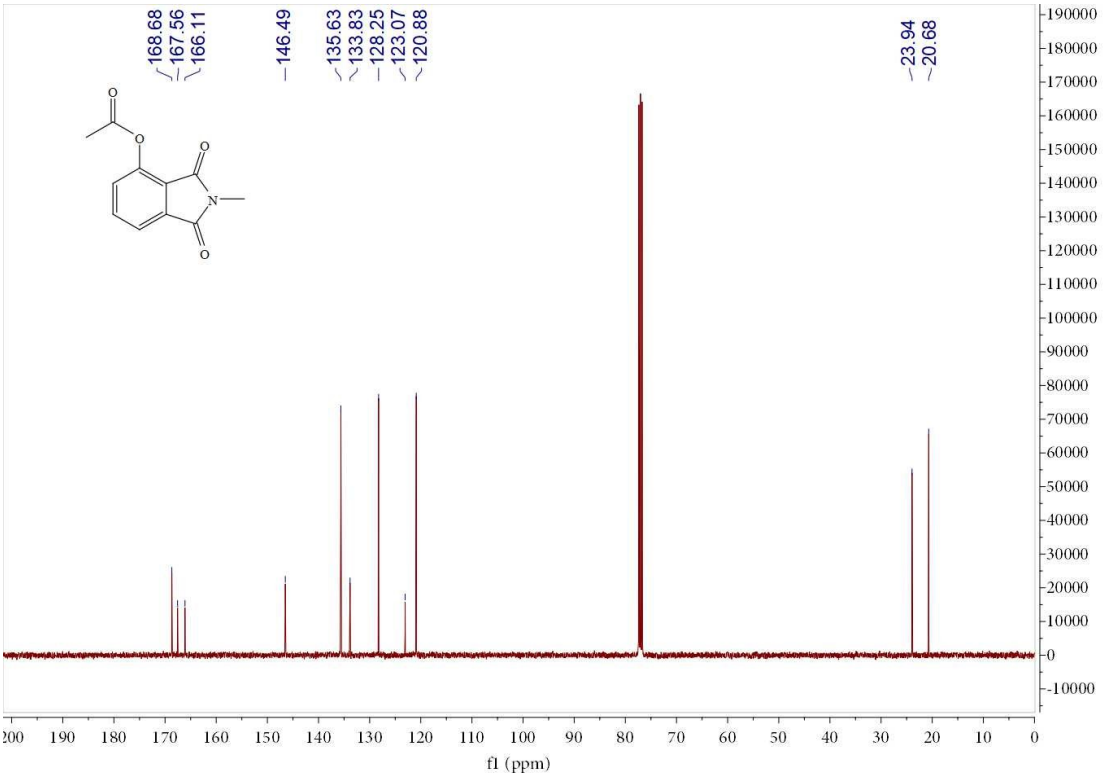

Fig.S45 ^{13}C NMR spectrum of compound **8b** (**PHI-6**).

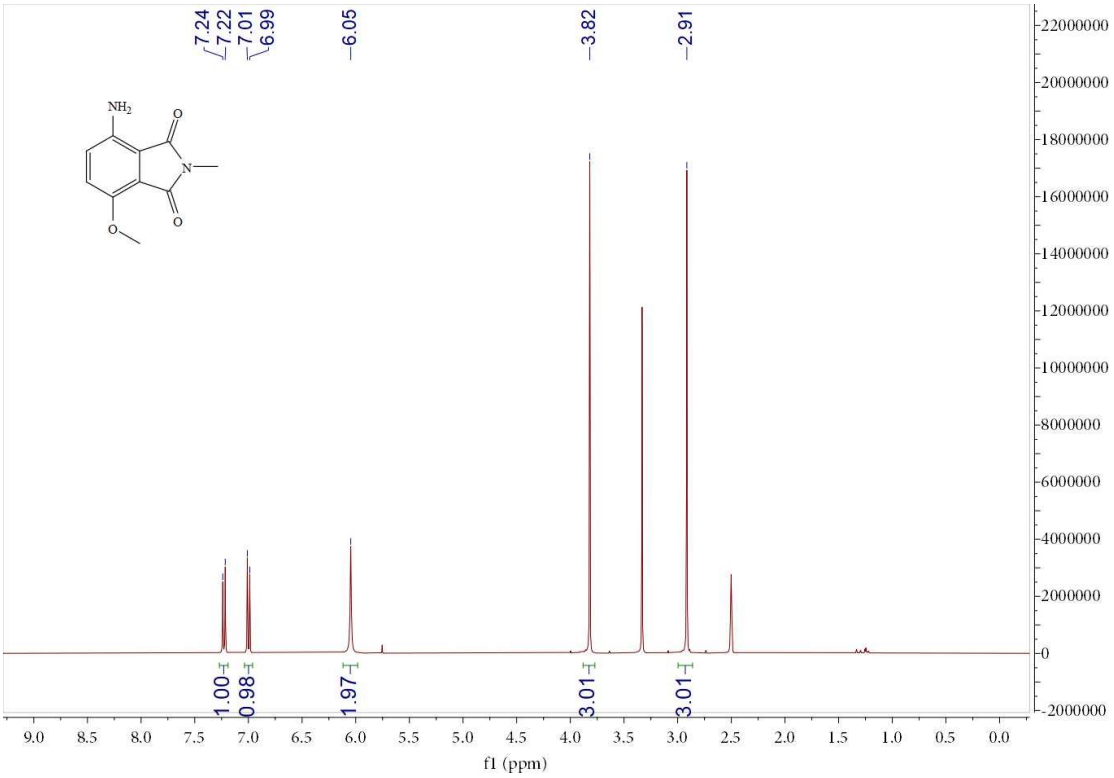

Fig.S46 ^{1}H NMR spectrum of compound **9** (**PHI-5**).

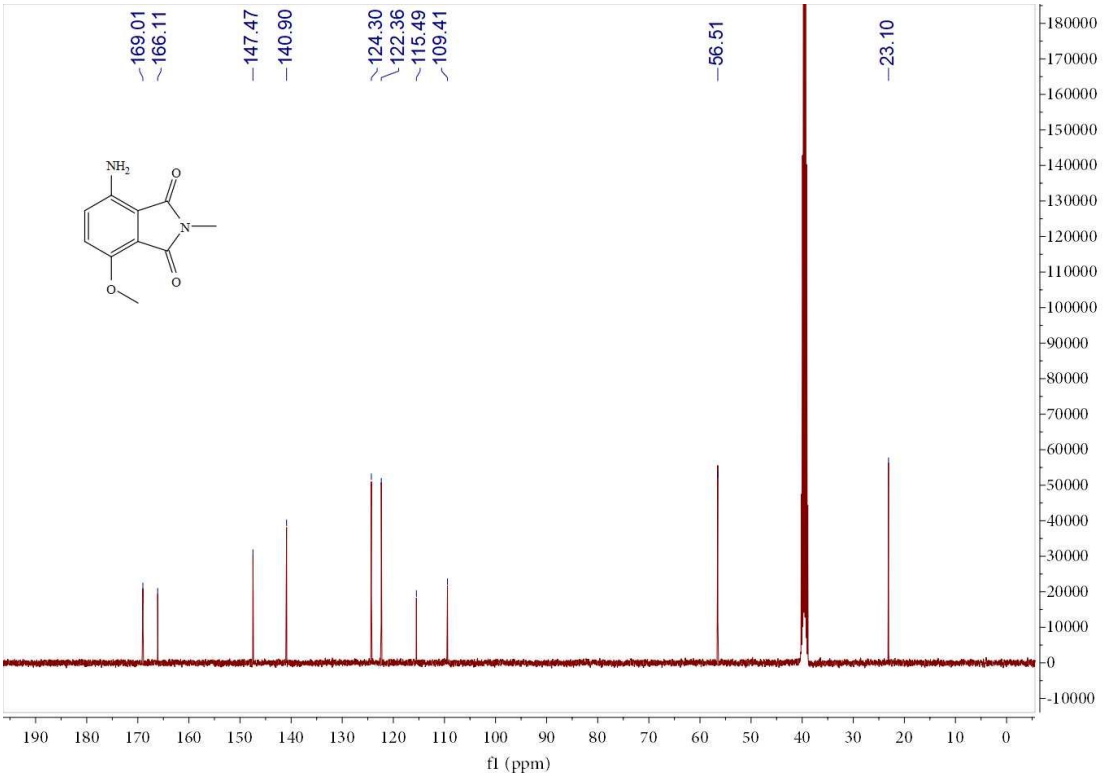

Fig.S47 ^{13}C NMR spectrum of compound **9** (**PHI-5**).

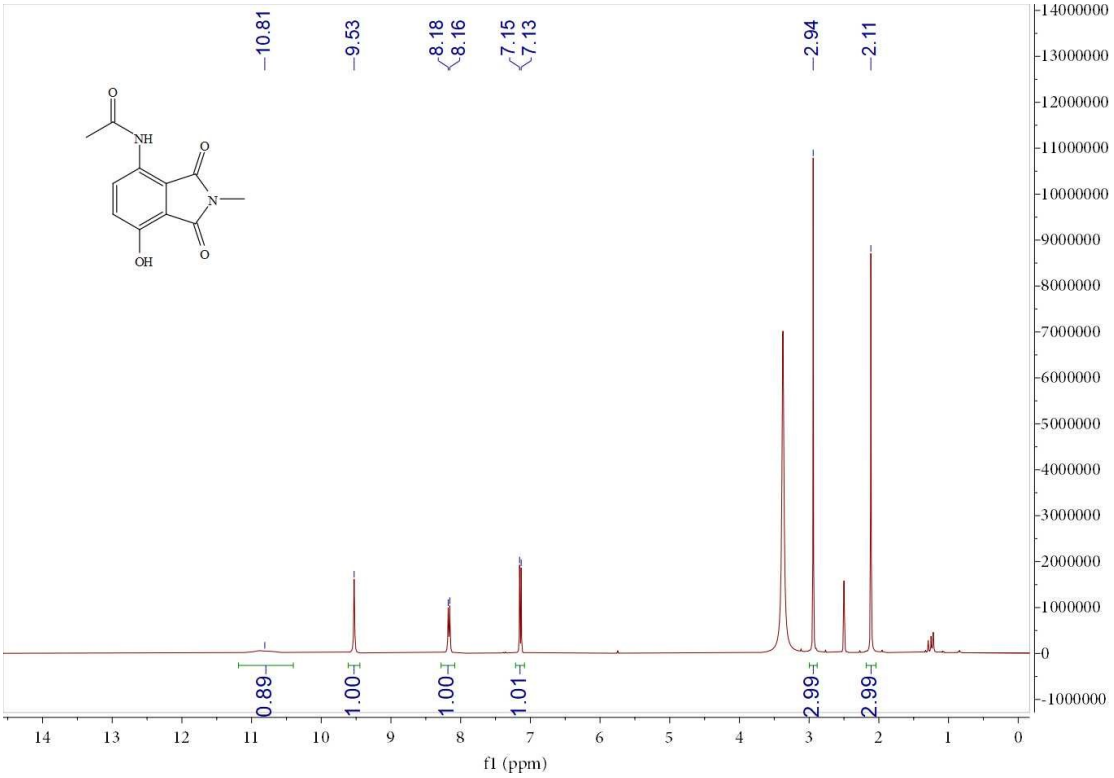

Fig.S48 ^{1}H NMR spectrum of compound **10** (**PHI-7**).

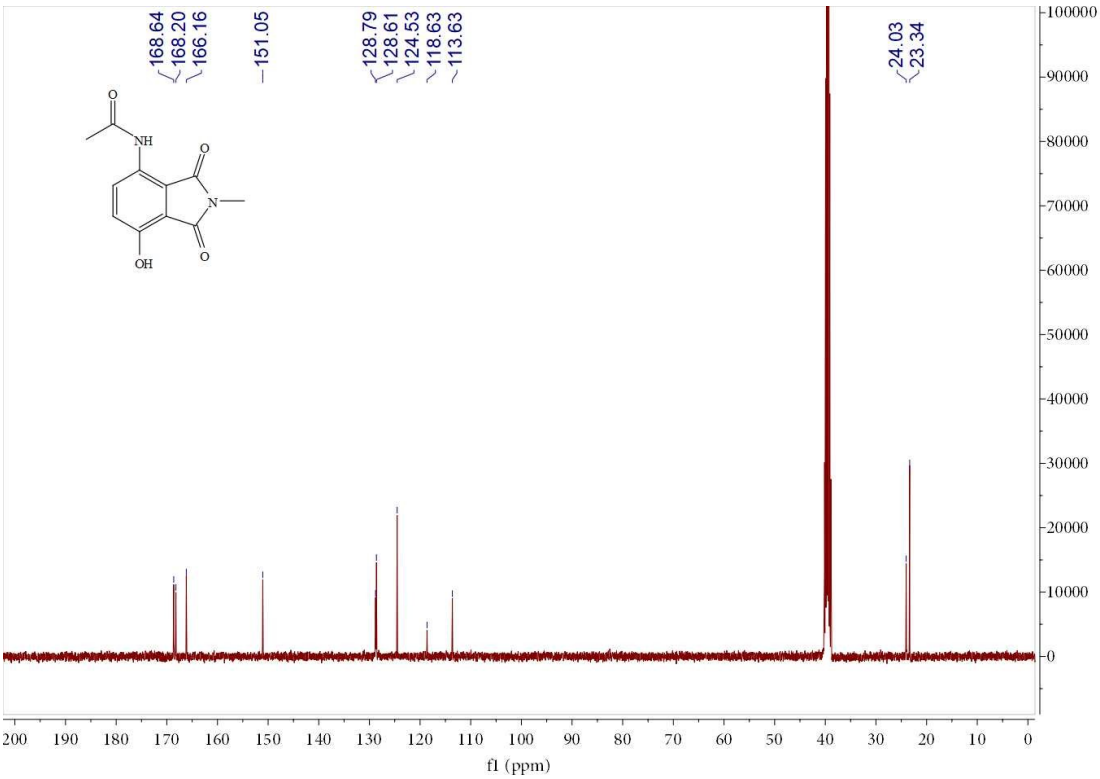

Fig.S49 ^{13}C NMR spectrum of compound **10** (**PHI-7**).

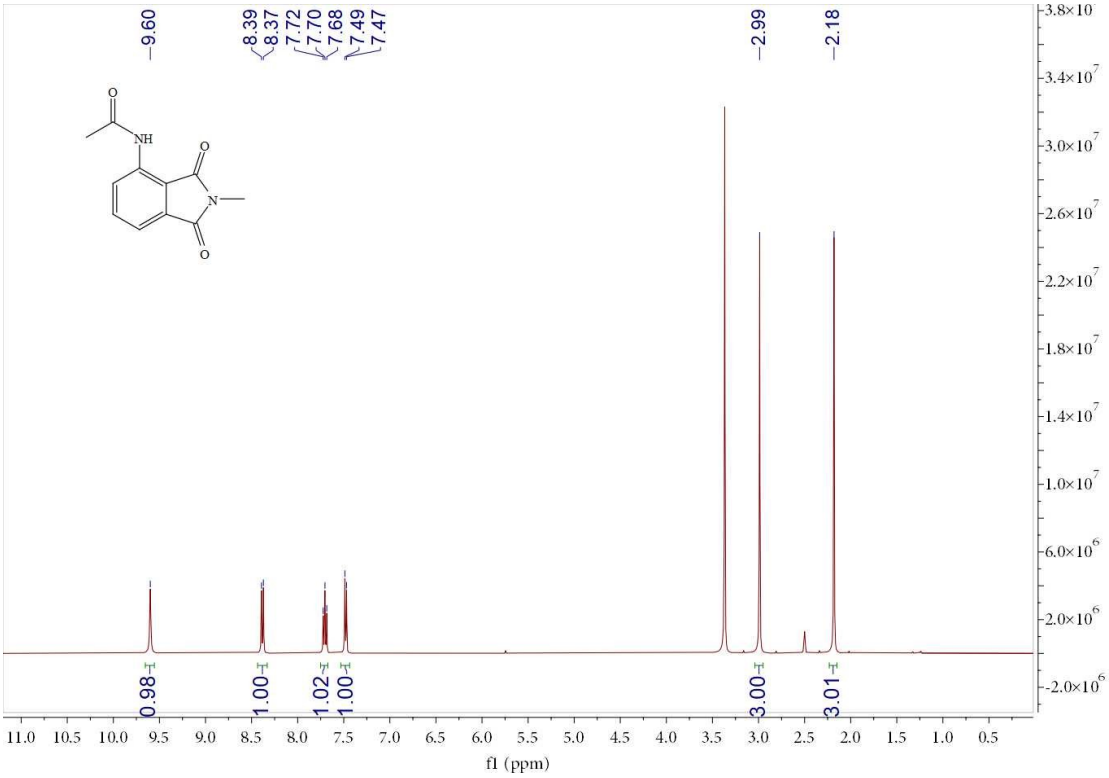

Fig.S50 ^{1}H NMR spectrum of compound **11** (**PHI-8**).

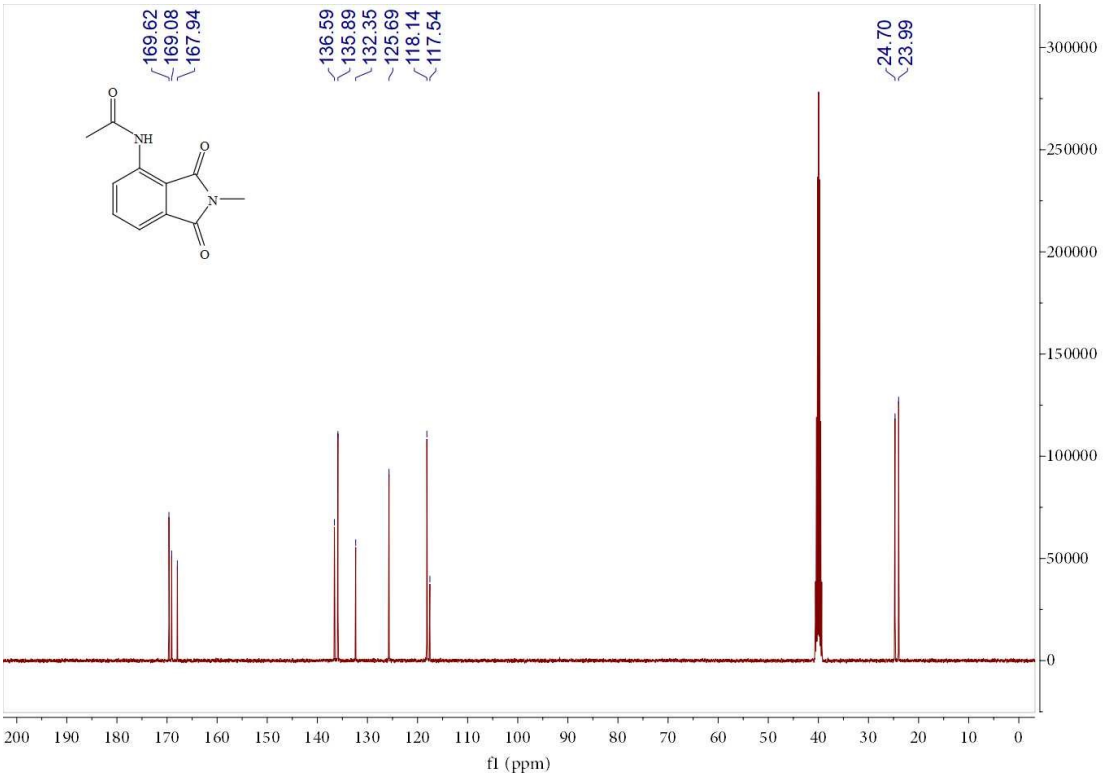

Fig.S51 ^{13}C NMR spectrum of compound **11** (**PHI-8**).

6. References

[1] Konev MO, Cardinale L, Jacobi von Wangelin A. Catalyst-Free N-Deoxygenation by Photoexcitation of Hantzsch Ester. Org Lett 2020;22:1316-20.

[2] Priessner M, Summers PA, Lewis BW, Sastre M, Ying L, Kuimova MK, Vilar R. Selective Detection of Cu(+) Ions in Live Cells via Fluorescence Lifetime Imaging Microscopy. Angew Chem Int Ed Engl 2021;60:23148-53.

[3] Paranawithana NN, Martins AF, Clavijo Jordan V, Zhao P, Chirayil S, Meloni G, Sherry AD. A Responsive Magnetic Resonance Imaging Contrast Agent for Detection of Excess Copper(II) in the Liver In Vivo. J Am Chem Soc 2019;141:11009-18.

[4] Tu HC, Chen HY, Wu CY, Lin PC. Responsive fluorescence enhancement for in vivo Cu(II) monitoring in zebrafish larvae. Biosens Bioelectron 2022;200:113885.

[5] Liu J, Liu Z, Wang W, Tian Y. Real-time Tracking and Sensing of Cu(+) and Cu(2+) with a Single SERS Probe in the Live Brain: Toward Understanding Why Copper Ions Were Increased upon Ischemia. Angew Chem Int Ed Engl 2021;60:21351-59.

[6] Yi XQ, He YF, Cao YS, Shen WX, Lv YY. Porphyrinic Probe for Fluorescence "Turn-On" Monitoring of Cu(+) in Aqueous Buffer and Mitochondria. ACS Sens 2019;4:856-64.

[7] Zhou Z, Chen S, Huang Y, Gu B, Li J, Wu C, Yin P, Zhang Y, Li H. Simultaneous visualization and quantification of copper (II) ions in Alzheimer's disease by a near-infrared fluorescence probe. Biosens Bioelectron 2022;198:113858.

[8] Zhang H, Feng L, Jiang Y, Wong YT, He Y, Zheng G, He J, Tan Y, Sun H, Ho D. A reaction-based near-infrared fluorescent sensor for Cu(2+) detection in aqueous buffer and its application in living cells and tissues imaging. Biosens Bioelectron 2017;94:24-29.

[9] Tang J, Ma S, Zhang D, Liu Y, Zhao Y, Ye Y. Highly sensitive and fast responsive ratiometric fluorescent probe for Cu2+ based on a naphthalimide-rhodamine dyad and its application in living cell imaging. Sensors and Actuators B: Chemical 2016;236:109-15.

[10] Park SY, Kim W, Park SH, Han J, Lee J, Kang C, Lee MH. An endoplasmic reticulum-selective ratiometric fluorescent probe for imaging a copper pool. Chem Commun (Camb) 2017;53:4457-60.

[11] Okamoto Y, Kishikawa N, Hagimori M, El-Maghrabey M, Kawakami S, Kuroda N. A turn-on hydrazide oxidative decomposition-based fluorescence probe for highly selective detection of Cu(2+) in tap water as well as cell imaging. Anal Chim Acta 2022;1217:340024.

[12] Zhou Z, Tang H, Chen S, Huang Y, Zhu X, Li H, Zhang Y, Yao S. A turn-on red-emitting fluorescent probe for determination of copper(II) ions in food samples and living zebrafish. Food Chem 2021;343:128513.

[13] Yamabe S, Zeng G, Guan W, Sakaki S. An aniline dication-like transition state in the Bamberger rearrangement. Beilstein journal of organic chemistry 2013;9:1073-82.

[14] Ng SM, Wu X, Khyasudeen MF, Nowakowski PJ, Tan HS, Xing B, Yeow EKL. Vancomycin Determination by Disrupting Electron-Transfer in a Fluorescence Turn-On Squaraine-Anthraquinone Triad. ACS Sens 2018;3:1156-63.